Biosensors and Bioelectronics 142 (2019) 111552

Contents lists available at ScienceDirect

Biosensors and Bioelectronics

journal homepage: www.elsevier.com/locate/bios

Emerging technologies for antibiotic susceptibility testing

Bhagaban Behera[a], Anil Vishnu G.K.[a,b], Suman Chatterjee[a], V.S.N. Sitaramgupta V[a], Niranjana Sreekumar[a], Apoorva Nagabhushan[a], Nirmala Rajendran[c], Prathik B.H.[d], Hardik J. Pandya[a,*]

[a] Biomedical and Electronic (10^{-6}-10^{-9}) Engineering Systems Laboratory, Department of Electronic Systems Engineering, Indian Institute of Science, Bangalore, India
[b] Center for BioSystems Science and Engineering, Indian Institute of Science, Bangalore, India
[c] IISc Medical Center, Indian Institute of Science, Bangalore, India
[d] Indira Gandhi Institute of Child Health, Bangalore, India

ARTICLE INFO

Keywords:
Bacteria
Antibiotics
AST
Emerging technologies
Microfabrication

ABSTRACT

Superbugs such as infectious bacteria pose a great threat to humanity due to an increase in bacterial mortality leading to clinical treatment failure, lengthy hospital stay, intravenous therapy and accretion of bacteraemia. These disease-causing bacteria gain resistance to drugs over time which further complicates the treatment. Monitoring of antibiotic resistance is therefore necessary so that bacterial infectious diseases can be diagnosed rapidly. Antimicrobial susceptibility testing (AST) provides valuable information on the efficacy of antibiotic agents and their dosages for treatment against bacterial infections. In clinical laboratories, most widely used AST methods are disk diffusion, gradient diffusion, broth dilution, or commercially available semi-automated systems. Though these methods are cost-effective and accurate, they are time-consuming, labour-intensive, and require skilled manpower. Recently much attention has been on developing rapid AST techniques to avoid misuse of antibiotics and provide effective treatment. In this review, we have discussed emerging engineering AST techniques with special emphasis on phenotypic AST. These techniques include fluorescence imaging along with computational image processing, surface plasmon resonance, Raman spectra, and laser tweezer as well as micro/nanotechnology-based device such as microfluidics, microdroplets, and microchamber. The mechanical and electrical behaviour of single bacterial cell and bacterial suspension for the study of AST is also discussed.

1. Introduction

Antibiotic resistance by pathogenic bacterial strains is a major prevalent health crisis in the world today. Antibiotics are drugs that can effectively kill (bactericidal antibiotics) or inhibit (bacteriostatic antibiotics) the growth of bacteria causing infections in both humans and animals (Nemeth et al., 2015). Alexander Fleming, a Scottish physician, is widely credited for the discovery of the world's first antibiotic (Penicillin G) from fungus Penicillium notatum in 1928. This discovery has saved the lives of millions of people across the globe from bacterial infections (Tan and Tatsumura, 2015). β-lactam antibiotics, a class of broad-spectrum antibiotics including I, II and III generation cephalosporins, monobactams, carbapenems, β-lactamase inhibitors, and penicillin are widely used in treating bacterial infections (Kong et al., 2010). Cephalosporins are widely used as intravenous antibiotics and fluoroquinolones are major oral antibacterial drugs used in the treatment of bacterial infections. Antibiotics are a widely used medication in treating global bacterial infections. There has been a significant rise in resistance to most commercially accepted antibiotics. A detailed understanding of bacterial resistance mechanisms will help for developing novel antibiotic testing platforms for rapid treatment of bacterial infections (Heesemann, 1993). It is known that the bacteria acquire resistance to antibiotics by producing extended spectrum β-lactamase enzyme (Soltani et al., 2014). The β-lactamase gene inactivates β-lactam antibiotics like penicillin and cephalosporins by hydrolyzing the β-lactam ring that plays a crucial role in inhibiting bacterial cell wall biosynthesis (Saravanan et al., 2018). Bacteria can mask the target drug and reprocess DNA mechanisms, develop mutations, and express alternative proteins. They can also protect their target sites from antibiotic action by modifying them. Certain enzymes produced by bacteria are capable of altering the antibiotic molecule by inducing chemical changes and thereby, destroying the molecule. In the case of gram-negative bacteria, drug uptake is prevented from permeating the inner cytoplasmic membrane (Munita and Arias, 2016). Antibiotic resistance

* Corresponding author.
E-mail address: hjpandya@iisc.ac.in (H.J. Pandya).

https://doi.org/10.1016/j.bios.2019.111552
Received 22 April 2019; Received in revised form 27 July 2019; Accepted 29 July 2019
Available online 09 August 2019
0956-5663/

can also be acquired by either horizontal transfer of resistant genes by conjugation, transformation, and transduction or vertical transfer by mutation among different bacterial strains (Read and Woods, 2014). In some cases, antibiotics are expelled out from the cells before it can reach the target location.

The life-threatening condition of a patient can be avoided by identifying correct bacteria causing the condition and the most effective antibiotic against this bacterium considering its resistance against antibiotics. Biosensors being highly sensitive, specific, repeatable, rapid, label-free, inexpensive, and compact are a preferred choice in developing point-of-care platforms for AST. A biosensor detects bacteria through a two-step process viz. i) biological recognition element to recognize pathogen of interest which may include antibodies, enzymes, whole cells, nucleic acids, receptors, aptamers, peptides or lipids, and ii) transducers to convert the biological signal generated by recognition element into a measurable electrical signal (Bhalla et al., 2016; Mehrotra, 2016; Turner, 2013). Currently, microbiological techniques like bioassays, screening methods including disk diffusion, antimicrobial gradient diffusion, broth dilution, and cell culture are some of the common methods adopted by health care facilities for measuring the effectiveness of antibiotics (Puttaswamy et al., 2018; Reller et al., 2009a). The rapid detection and identification of pathogenic bacteria that are typically present in low concentrations in patient samples is the limitation of these methods. Such typical bacterial growth and susceptibility testing require more than 24 h to obtain results. In the current scenario, accurate, evidence-based, and targeted antibiotic prescribing by clinicians are problematic and hence they are forced to prescribe broad-spectrum antibiotics. Thus, there is a pressing need for highly sensitive, specific, repeatable, rapid, label-free, inexpensive, and compact point-of-care platforms for antimicrobial susceptibility testing (AST). AST profiling are performed in two ways: genotypic and phenotypic based methods. Genotypic methods, though rapid and accurate, are however limited by their cost, labour intensiveness, and difficulty in translating into point-of-care platforms in many cases (Nseir and Povoa, 2015; Schofield, 2012). Phenotypic methods, through their fundamental interactions with the physical environment, provide more avenues for emerging engineering technologies to be applied to them to improve their efficiency and versatility. In this review, we provide an overview of different approaches for phenotypic AST developed over the years after a brief discussion on conventional AST techniques. We have primarily focused on devices/tools such as, microcalorimetry, flow cytometry, microfluidics, microcantilever technology, high-frequency electromagnet sensor, pH sensor, mass spectrometry, capacitance sensor, nuclear magnetic resonance, microsound detection, Raman spectroscopy, semiconductor quantum well, fluorescence detection, and impedance methods to measure AST profile in terms of simplicity, cost-effectiveness, and low processing time. The key techniques discussed have been graphically portrayed in Fig. 1 and their highlights have been summarized in Table 1. The publication statistics for articles on antibiotic or antimicrobial susceptibility testing is shown in Electronic Supplementary Information (ESI) along with a figure depicting past, present and future trends in AST.

2. Classical and commercial AST

Conventional ASTs are based on bacterial growth with and without antibiotics on a solid agar plate or in a liquid growth medium. The test is carried out on agar plate by identifying inhibition zones after culture whereas, in liquid-based methods, change in optical density is measured. Several successful results have been achieved using this method while testing on different bacteria and antibiotics (Reller et al., 2009b, 2009a; Syal et al., 2017a). In the disk diffusion method, a disk impregnated with antibiotic drug is placed on an agar plate which is coated with the test bacterium (Reller et al., 2009c). Then the plate is incubated overnight to allow the antibiotic to diffuse from the filter paper into the agar. If an antibiotic is effective, it stops the bacteria to grow around the antibiotic disk or kills the bacteria around the disk forming a clear, visible ring around the disk. The diameter of the growth area is a direct measure of the susceptibility of the bacteria to the antibiotic. The advantages of disk diffusion process are its simplicity, cost-effectiveness, and easy interpretation. However, the main disadvantage of this process is that it needs manual processing and lacks automation. Further, this process provides only qualitative and not quantitative results. Additionally, disk diffusion has been employed in different ways to study AST. Khatoon et al. used silver nanoparticles (AgNPs) in place of conventional drugs to study AST using disk diffusion (Khatoon et al., 2017). Similarly, the antibacterial activity of alginate films incorporated with graphene oxide was studied using disk diffusion method (Frígols et al., 2019). AST using agar and broth dilution is one of the oldest methods used to determine the minimum inhibitory concentration (MIC). In the agar dilution method, a known number of bacterial cells are marked as a spot on an agar plate containing different concentrations of antibiotic (Balouiri et al., 2016a; Reller et al., 2009c). After incubation, the spots are examined for bacterial growth. The agar dilution method is capable of testing one antibiotic at a time whereas more than one antibiotic can be tested at once in broth dilution. In the broth dilution method, antibiotics are diluted two folds in a liquid growth medium and incubated after inoculation with a standard bacterial suspension. Post incubation samples are examined to find out MIC. This method is also used to measure time-kill i.e. rate of bacterial death for different concentration of drugs over a period of time up to 24 h (Gupta et al., 2015). The advantages of these dilution processes are reproducibility and cost-effectiveness. However, it is labour-intensive and expensive in nature. A nearly similar technique called microbroth dilution is now employed to reduce reagents and processing time. The antimicrobial gradient method also called E-test combines the principles of both dilution and diffusion methods to determine the minimum inhibitory concentration (MIC) of the drug (Belkum and Dunne, 2013; Citron et al., 1991; Puttaswamy et al., 2018; Reller et al., 2009b, 2009a). This method provides direct quantification of AST by dilution and diffusion of antibiotic in an agar plate. The process relies on creating a predefined, continuous concentration gradient of the antibiotic to be tested in an agar medium to determine susceptibility. In this procedure, an antibiotic-soaked strip is taken with an increasing concentration gradient from one end to the other and is deposited on the agar surface. The intersection of the growth inhibition ellipse and the strip is determined as the MIC value of the drug (Balouiri et al., 2016a; Reller et al., 2009c). This process is simple to implement and thus, is regularly used. However, E-test is not cost effective for large-scale AST measurement of multiple drugs. A good correlation between the MIC values obtained through broth dilution or agar dilution method and E-test has been reported (Baker et al., 1991; Berghaus et al., 2015; Gupta et al., 2015). E-test can also be used to investigate the antibacterial effect when multiple drugs are used (White et al., 1996). To profile AST of two antibiotics on a sample simultaneously, an E-test strip soaked with the first antibiotic is placed on an agar plate coated with the bacteria under study. Another strip soaked with the next antibiotic is used to replace the first strip after 1 h. In the commercial version of E-test, 5–6 strips can be placed radially on the surface of an agar plate coated with bacteria. After overnight incubation, a growth inhibition area, in the shape of an ellipse, at the immediate vicinity of the test strip can be observed and MIC can be determined from this observation (Jorgensen and Ferraro, 2009). E-test is also used to test critical samples like blood and cerebrospinal fluid (CSF) with both gram-positive and gram-negative bacteria. The MIC value in μg/mL range can be observed at the ellipse edge that intersects the strip. The advantages of this method are easy test procedures, able to determine contamination, and ability to test fastidious organisms which are not reliable in disk diffusion methods. However, E-test is relatively expensive compared to disk diffusion and dilution methods. In comparison, liquid suspension-based methods are faster than those based on solid-state medium owing to increased growth rate

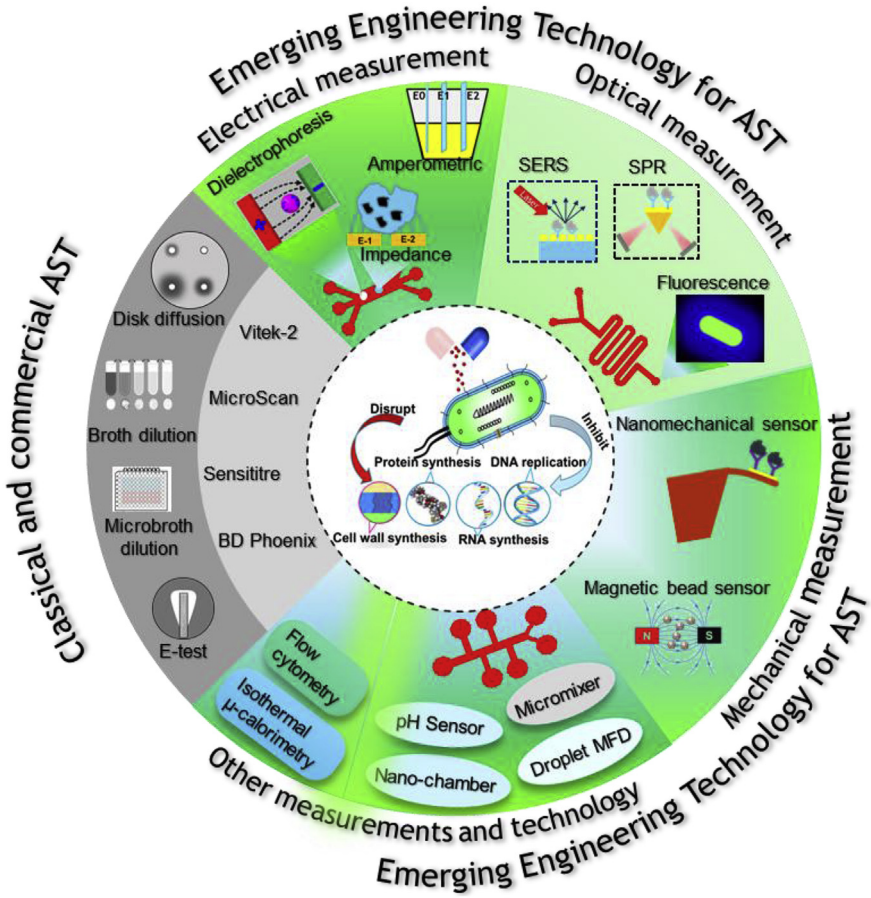

Fig. 1. Highlights of different techniques for AST applications.

capabilities. But liquid suspension-based methods are more laborious than solid state ones. To address this problem, several instruments like Phoenix (made by Becton-Dickinson, Franklin Lakes, NJ), Microscan (made by Beckman Coulter, Brea, CA), Sensititre (made by Thermo Scientific Waltham, Massachusetts, USA) and Vitek-1/Vitek-2 (made by bioMérieux, Marcy-L'Etoile, France) have been developed for high throughput AST. BD Phoenix is based on turbidity reading and colorimetric change. This system can use up to 99 panels (cassettes) and provide results in ~6–16 h. Similarly, Microscan uses 96-well microdilution tray and is capable of handling more than 40 trays at a time. In this system, AST is examined by recording bacterial turbidity using a specialized photodetector and typical process time is ~4.5–18 h. Sensititre uses 96-well plates and is capable of handling 64 plates. In this instrument, bacterial growth is monitored by measuring fluorescence intensity and the typical process time is over 18 h. The Vitek AST instrument uses 64 well plate and can handle up to 240 plates by providing results over 4 h. The major limiting factor of these commercial systems is the need to culture large concentrations of bacteria for a sufficiently long time to faithfully detect antibiotic effects on bacterial growth.

However, these systems strictly follow the Clinical and Laboratory Standards Institute (CLSI) and European Committee on Antimicrobial Susceptibility Testing (EUCAST) guidelines for antimicrobial susceptibility testing which comes across as a big advantage. Though these instruments are compatible with a wide spectrum of bacteria and antibiotics, they cannot handle polymicrobial bacteria and their corresponding antibiotics. The turbidity method has the uncertainty that it assumes bacterial growth and absorbance plot as linear. Also, these instruments are prohibitively expensive to use in a low-resource setting.

3. Engineering technologies for AST

3.1. Flow cytometry AST

Flow cytometry is a technique where optical and fluorescence characteristics are employed in cell counting, cell sorting, chromosome preparation, and biomarker detection by suspending them in a stream of fluid and passing them in front of a detector (Adan et al., 2017). Cell morphology and cell counts are measured by considering light scattering and excitation/emission spectra from different fluorescent materials such as FRET dyes, fluorophores or fluorescent proteins. In the context of AST it is known that antibiotics induce changes in different morpho-functional and physiological characteristics like membrane potential, cell size, cytoplasmic membrane integrity, and amount of DNA (Adan et al., 2017; Chaturvedi et al., 2004; Jepras et al., 1997; Tracy et al., 2010). This is leveraged in the methods that use flow cytometry to perform AST. This enables faster processing as compared to conventional methods as changes in physiological parameters caused by antibiotics is faster than growth inhibition processes (1–2 h vs 16–24 h). A comparative study of AST using flow cytometry-based and conventional techniques by Gauthier et al. showed 93.9% accuracy (Gauthier et al., 2002). This method has been applied to several bacterial species and combinations of antibiotics by using various dye/fixation combinations (Chaturvedi et al., 2004; Faria-Ramos et al., 2013; Gauthier et al., 2002; Huang et al., 2015; Jepras et al., 1997). Although flow cytometry can produce AST results within few hours, it has not been used significantly due to inefficiency for complex patient samples, staining inefficiency of dyes, autofluorescence of certain bacterial creating noise, and unable to differentiate the effect of bactericidal or bacteriostatic antibiotics. Additionally, verification and validation of the clinical database require an enormous amount of work to

Table 1
Summary of conventional and emerging engineering AST technologies.

Methods	Antimicrobial testing technology	Test principle	Automatic/ Manual	Test time (h)	Bacteria tested	Cost	MIC detected	Features	Ref.
Traditional	Disk diffusion	Filter paper containing antibiotic of desired concentrations are placed on agar surface which is coated with bacteria	Manual	16–24	Almost all kind of bacteria and yeast	Low	Yes (not consistent)	Simple interpretation, approved by CLSI, labor-intensive, high detection limit, and MIC determination is not consistent	(Bauer et al., 1966, 1959; Reller et al., 2009a)
	Agar dilution	Different concentrations of antibiotics added to agar plates and bacteria coated on the surface	Manual	16–24	Almost all kind of bacteria	Low	Yes	Approved by CLSI, and simple interpretation, labor-intensive, slow and high detection limit	(Baker et al., 1991; Balouiri et al., 2016a, 2016b; Berghaus et al., 2015; Gupta et al., 2015)
	Broth dilution or Broth microdilution	Different concentrations of antibiotics are added to bacterial culture media	Manual	16–24	Almost all kind of bacteria	Low	Yes	Appropriately determines MIC, approved by CLSI, labor-intensive and requirement of high reagent volume	(Baker et al., 1991; Balouiri et al., 2016b; Berghaus et al., 2015; Jorgensen and Ferraro, 2009; Reller et al., 2009a)
	E-test	A strip soaked with gradient concentrations of antibiotic kept on agar surface which is coated with bacteria	Manual	12–20	Almost all kind of bacteria	Medium	Yes	MIC determination, easy interpretation, approved by CLSI, labor-intensive, expensive as compared to other classical techniques	(Baker et al., 1991; Berghaus et al., 2015; Mittman et al., 2009; White et al., 1996)
Commercial instruments	Flow cytometry	Cells viability are counted with the help of dyes	Semi-automatic	2–6	Almost all kind of bacteria	High	Yes	semi-Automated, and relatively simple, low detection limit, and expensive	(Faria-Ramos et al., 2013; Gauthier et al., 2002; Huang et al., 2015; Ramani et al., 1997; Saint-Ruf et al., 2016)
	Isothermal microcalorimetry	Measures heat flowrate (which is proportional to physical or chemical change) of bacterial suspension in the presence or absence of antibiotics	Automatic	~24	Almost all kind of bacteria	Medium-High	Yes	Safe to operate even to high-risk bacteria, time-consuming and can't determine the exact nature of physical or chemical change	(Bonkat et al., 2013; Braissant et al., 2009; Howell et al., 2012; Lewis and Daniels, 2003; Nawattanapaiboon et al., 2015; Tafin et al., 2012; von Ah et al., 2009)
	Sensititre	Fluorescence measurement of enzymatic activities of bacterial suspension in the presence of antibiotics	Automatic	18–24	Almost all kind of bacteria and yeast	Medium-High	Yes	Sensitive, relatively inexpensive, approved by CLSI, time-consuming	(Alexander et al., 2007; Cuenca-Estrella et al., 2010; Espinel-Ingroff et al., 1999)
	Vitek-1/Vitek-2	Measure bacterial growth in the presence of antibiotics by recording light attenuation using a photometer	Automatic	6–24	Almost all kind of bacteria	Medium-High	Yes	Sensitive, relatively inexpensive, and approved by CLSI, time-consuming and not suitable for POC applications	(Cuenca-Estrella et al., 2010; Eigner et al., 2005; Jiang et al., 2016; Mittman et al., 2009)
	BD Phoenix	Recording of bacterial suspension turbidity and colorimetric changes in the presence of antibiotics	Automatic	4–16	Almost all kind of bacteria	Medium-High	Yes	Sensitive, and relatively inexpensive, approved by CLSI, time-consuming	(Eigner et al., 2005; Mittman et al., 2009; Snyder et al., 2008)
Mechanical	Asynchronous magnetic bead rotation sensor	Measurements of magnetic beads rotational frequency	Semi-automatic	1–6	*E. coli*	High	Yes	Highly sensitive, single bacteria observation, not tested with other bacteria, and system is complex	(Kinnunen et al., 2012, 2011; Sinn et al., 2012, 2011)
	Cantilever	Measurement of cantilever fluctuations by placing bacteria cells on it	Semi-automatic	~2	*E. coli, S. aureus*	High	Yes	Highly sensitive, complex fabrication process and complex measurement	(Etayash et al., 2016; Gfeller et al., 2005; Lissandrello et al., 2014; Longo et al., 2013)
	Crystal resonator	Measurement of change in resonant frequency	Semi-automatic	15 min-2 h	*E. coli, E. faecalis*	High	No	Highly sensitive, and complex measurement	(Cermak et al., 2016; France et al., 2016; Johnson et al., 2017)
Optical	Surface plasmon resonance	Measurement of refractive index	Automatic	~2	*E. coli, S. epidermidis, MRSA, MSSA*	High	Yes	Sensitive, fast, complex	(Chiang et al., 2009; Tawil et al., 2013)
	SERS	Measurement of Raman scattered light signals with the help of metallic nanoparticles	Automatic	~2	*E. coli, K. pneu, S. sapro, E. faecalis*	High	Yes	Sensitive, fast, moderately complex, expensive, Complex algorithm needed	(Chabot et al., 2013; Galvan and Yu, 2018; Liu et al., 2016, 2009; Martinez-Perdiguero et al., 2013; Premasiri et al., 2017, 2017)

(*continued on next page*)

Table 1 (*continued*)

Methods	Antimicrobial testing technology	Test principle	Automatic/ Manual	Test time (h)	Bacteria tested	Cost	MIC detected	Features	Ref.
	Laser tweezers	Raman spectra study of optically trapped bacterial cell's surface	Automatic	~4	*E. coli*	High	Yes	Sensitive, Fast, characterize single cell, moderately complex, Expensive, Complex algorithm needed	(Moritz et al., 2010a; Pilát et al., 2018; Samadi et al., 2015)
	Phase shift Spectroscopy	Optical (reflectance) study of Si micropillar topologies and colonized bacteria in suspension	Automatic	2–3	*E. coli*	High	Yes	Sensitive, fast, real-time, complex, expensive, complex data accusation	Leonard et al. (2017)
Electrical	Impedance	Impedance measurement of bacterial suspension	Semi-automatic	0.5–1.5	*E. coli, MRSA*	Medium	Yes	Simple, rapid, real-time, inexpensive, miniaturized	(Puttaswamy et al., 2012; Safavieh et al., 2017)
	Capacitance	Capacitance measurement of bacterial suspension	Manual	2.5	*E. coli, S. thyphi, P. aeruginosa, S. epidermidis, S. aureus, B. subtilis*	Medium	Yes	Simple, real-time, inexpensive miniaturized	(Jo et al., 2018; Niyomdecha et al., 2017)
	Electrochemical	Measurement of change in current due to electrochemical reactions	Manual	1	*E. coli*	Low-Medium	Yes	Rapid, Inexpensive, Moderately complex, chemical wastage	(Ertl et al., 2000; Mann and Mikkelsen, 2008; Onishi et al., 2018)
Engineering approaches	Gradient MFD	Concentration gradient formed on the chip by various design	Semi-automatic	2.5–4	*P. aeruginosa, E. coli, S. aureus, Salmonella typhimurium*	High	Yes	High throughput, multiple antibiotics with different concentration can be tested in one shot. complex design	(Derzsi et al., 2016; Hou et al., 2014b; Kim et al., 2015; Li et al., 2014)
	pH Sensor	Measurement of effective optical thickness of porous silicon embedded pH sensitive material	Semi-automatic	2	*E. coli*	High	Yes	Rapid, no long-term pre-incubation required, small sample volume, expensive equipment requirement,	Tang et al. (2013)
	Microfluidic agarose channel	Bacteria immobilized in agarose and monitored using microscope	Semi-automatic	4–10	206 bacteria tested by (Choi et al., 2017)	Medium	Yes	Small sample volume, Real-time, relatively slow, inexpensive equipment requirement,	(Choi et al., 2017, 2016, 2013)
	Droplet microfluidics	Monitoring of growth of bacterial by confining them in a nanolitre volume	Automatic	3	Different bacteria	Medium	Yes	Rapid, automated, Single bacteria can be studied, small sample volume, high throughput, multiplexing possible, expensive equipment requirement, complicated chip design	(Chung et al., 2016; Jiang et al., 2016; Kaushik et al., 2017; Sabhachandani et al., 2017; Sinn et al., 2011)
	Dielectrophoresis induced AST	Monitoring dielectrophoretic behaviour of elongated bacteria	Semi-automatic	1.5–4	*P. aeruginosa, E. coli, K. pneumoniae*	Medium	Yes	Fast, high throughput, multiplexing possible	(Braff et al., 2013; Chung et al., 2012, 2011; Peitz and van Leeuwen, 2010; Su et al., 2017)
	Stress-Induced AST	High flow rates on-chip stress immobilized bacteria in the presence and absence of antibiotic; number of dead bacteria tracked via microscopy	Semi-automatic	1–2	*S. aureus, E. cloacae, E. coli, K. pneumoniae, P. aeruginosa*	High	Yes	Effective, rapid, high throughput, expensive, chances of leakage during testing, high sample volume required	(Kalashnikov et al., 2018, 2017, 2014, 2012)

be certified by CLSI (van Belkum and Dunne, 2013).

3.2. Isothermal microcalorimetry (IMC)

Isothermal microcalorimetry (IMC) enables heat flow measurement, which is directly related to physical or chemical processes (based on the metabolic activity of growing bacteria). In IMC, a microorganism containing glass ampoule is placed in a measuring channel and heat flow is continuously measured. These continuous signals of heat flow are evaluated and calibrated with the amount of heat being produced in the ampule. IMC experiment is designed in such a way that observed heat flow is directly related to the process of interest by considering exothermic and endothermic reactions in the ampoule (Lewis and Daniels, 2003). For example, growth of *Escherichia coli (E. coli)* in M9 medium containing glucose and lactose as carbon sources induces metabolic activities such as glucose respiration, glucose fermentation, and lactose fermentation. Heat production from each metabolic process is calculated and evaluated by measurement data (Braissant et al., 2009). Instead of large volume ampule, researchers have developed chip microcalorimeters which use only a few micro/nanolitre of biological samples (Johannessen et al., 2002; Lee et al., 2009). This chip calorimeter has a heat power sensor developed using Micro Electromechanical Systems (MEMS) technology where all essential components like conductance sensor, heat sink, temperature sensors, heating resistors, and sample containers are integrated on a single chip (van Herwaarden, 2005). IMC has several advantages such as: (i) testing in sealed ampules, assuring safety towards high-risk bacteria, (ii) no manual manipulation of ampoules is needed, and (iii) antimicrobial activity can be calculated during the lag phase which cuts down on the wait time of measurement. Some of the limitations of this method are: (i) it requires reference sample at the desired temperature, (ii) AST measurement is carried out in a closed ampoule where environmental parameters such as oxygen concentration available may change over time, and (iii) non-specific heat flow may create problems. Overall, IMC shows fast and quantitative AST performance at an affordable price.

3.3. Optical density (OD) measurement

Optical density measures the concentration of bacteria in a suspension. When a light beam passes through a bacterial suspension, the scattered light detected by a spectrophotometer is correlated with bacteria density in colony-forming units (CFU). OD measurement of a bacterial suspension with antibiotics added can delineate between resistant and sensitive strains (Friedman et al., 2011). This method provides AST results in a few hours. However, it can neither calculate MIC nor it is suitable for low concentrations of bacterial suspension.

3.4. Raman spectroscopy

Raman spectroscopy is employed to measure molecular vibrations and thus is a useful technique to study biomolecules. In Raman spectroscopy intensity and wave number of in-elastic scattered light is measured. However, Raman spectra signals from biological samples are weak which limits its application. To work around this shortcoming, several research groups have combined Raman spectra and machine learning approaches (discriminant analysis) to differentiate between live and dead bacteria (Athamneh et al., 2014; Kastanos et al., 2010; Moritz et al., 2010b; Walter et al., 2011). Alternately, the weak Raman signals are amplified by using metallic nanoparticles (plasmon resonant particles such as silver (Ag), gold (Au)) through the process called Surface-Enhanced Raman Spectroscopy (SERS). The efficiency and sensitivity of SERS has also been further improved through the use of covalently bounded fragmented antibodies conjugated with the nanoparticles(Baniukevic et al., 2013). The use of antibodies in AST improves the capture efficiency of bacteria. SERS has been applied in several bioanalytical processes including bacterial identification and their characterization in the presence of antibiotics (Galvan and Yu, 2018). Liu et al. have demonstrated SERS based AST of *E. coli* and *S. aureus* using an array of Ag-nanoparticles imbedded in nanochannels of anodic aluminium oxide (Liu et al., 2009). In this case, the characteristic peaks of *S. aureus* and *E. coli* cell wall at 730 cm^{-1} and 1330 cm^{-1} respectively were studied in the presence of lysostaphin and lysozyme. The destruction of cell walls due to these antibiotics shifts the positions of these peaks significantly. The same team has extended this work to quantify MIC of oxacillin and imipenem when MSSA and wild-type *E. coli* were treated with these antibiotics respectively by measuring the intensities of specific biomarker peaks (Liu et al., 2016). The characteristic peak intensities at 730 cm^{-1} of *S. aureus and* 654 cm^{-1} of *E. coli* without (taken as reference) and with antibiotics were calibrated to find out MIC. In 2016, Hadjigeorgiou et al. performed AST of *Klebsiella pneumoniae, 16 Proteus,* and *E. coli* using SERS followed by the machine learning method known as Linear Discriminant Analysis (LDA) and Leave-One-Out Cross Validation (LOOCV) PC transformation (Hadjigeorgiou et al., 2016). This method could differentiate between resistant, intermediate, and sensitive bacteria with 94% correct classification. Similarly, Premasiri et al. studied 2 bacterial strains using SERS and applied the post partial least squares-discriminant analysis machine learning technique (Premasiri et al., 2017). This method provided resistant and susceptible bacteria with > 95% sensitivity and > 99% specificity. SERS-based AST is a label-free and non-invasive method.

3.5. Laser tweezers

The study of biological samples using Raman spectra was extended through a method called Laser Tweezers Raman spectroscopy (LTRS). In LTRS, individual cells are trapped in a laser focal volume using a Gaussian laser beam. LTRS provides unique advantages as it allows to characterize single cells in terms of bacterial identification and their metabolic activity. Moritz et al. have developed an inverted microscope having a laser source of wavelength 785 nm for LTRS study of *E. coli* (Moritz et al., 2010a). In this study, at a given time an average of five bacterial cells were captured. The Raman spectra intensities in range 710–1280 cm^{-1} of the trapped bacterial cells were studied over incubation time. Principal component analysis (PCA) was used as a machine learning technique to differentiate bacteria under normal and antibiotic influenced growth. Recently, Pilát et al. have used an optofluidic platform to manipulate single cell using LTRS after transferring individual bacteria cell into the microchambers (Pilát et al., 2018). In this LTRS system, individual cells were placed in micro-chambers with the help of optical tweezer and antibiotics induced morphological changes were evaluated using Raman spectra and post PCA computation. In another study, Samadi et al. used a 1064 nm laser beam to trap *E. coli* and studied the motility of the flagella in the presence of ethyl alcohol (Samadi et al., 2015). The killing time of *E. coli* was calculated using statistical analysis of power spectral density and their auto-correlation function. LTRS is generally applied in cases where the bacterial cell immobilizes upon antibacterial treatment owing to reduced availability of cellular energy for flagellar movement in comparison to normal healthy cells. This difference in motility is detected using this technique.

3.6. Surface Plasmon Resonance (SPR)

Surface Plasmon Resonance (SPR) is a physical process in which electron attached to the metal surface oscillates (at the metal-dielectric interface) under the influence of plane-polarized light. Since the oscillations of electrons are extremely sensitive to the refractive index of the dielectric, the change in the refractive index is measured when biomolecules are attached to the metal surface. SPR biosensors are label-free, ultra-sensitive, and allows for real-time detection (Lee et al., 2015; Martinez-Perdiguero et al., 2013; Nath and Chilkoti, 2004). In most

known applications, SPR is used to detect and identify cells, bacteria, or viruses based on affinity (Abdulhalim et al., 2008; Bai et al., 2012; Chabot et al., 2013; Firdous et al., 2018; Piliarik et al., 2009; Yanase et al., 2014). In 2009, Chiang et al. used SPR platform to test *E. coli* with ampicillin and *S. epidermidis* with tetracycline qualitatively (Chiang et al., 2009). In this study, one side of a prism was coated with a thin gold layer to increase the phase of the propagating optical wave. Ampicillin strongly affects the synthesis of the cell wall of *E. coli* JM109 and to detect this effect, the refractive index of cells near the cell-gold interface is measured. A significant SPR angle shift of susceptible strain and resistant strain of *E. coli* was observed. Also, significant SPR angle shift was observed when the susceptible and resistant strain of *S. epidermidis* was treated with tetracycline (a protein synthesis inhibitor). Similarly, Tawil et al. have studied on methicillin-resistant, methicillin-susceptible and borderline oxacillin-resistant *S. aureus* (Tawil et al., 2013). In this study, genomic DNA was extracted from *S. aureus* and amplified using the PCR technique and further evaluated using SPR by detecting specific penicillin-binding protein. Similarly, Nawattanapaiboon et al. have studied methicillin-resistant *S. aureus* by employing SPR imaging as a DNA biosensor (Nawattanapaiboon et al., 2015). On the other hand, Syal et al. have studied a unique phenotype AST method using plasmonic imaging and tracking (PIT) of *E. coli* O157:H7 as shown in Fig. 2(I) (Syal et al., 2017b, 2016). This plasmonic imaging setup used a high numerical aperture objective (NA 1.49) and an inverted microscope for contrast imaging of 47 nm thick gold sensor chip. The motion of individual bacterial cells was tracked with nanometer precision by considering the contrast change of plasmonic image. The action of antibiotic over period slows down nanoscale motions of the bacterial cell, which was tracked by the plasmonic imaging technique. In another scenario, Kee et al. used a plasmonic nanohole-based biosensor for monitoring growth of *E. coli* and evaluating AST performance (Kee et al., 2013). Plasmonic nanoholes were fabricated using standard microfabrication processes involving thermal oxidation, low-pressure chemical vapor deposition (LPCVD), lithography, sputtering, and etching. A photonic crystal-like structure with different through-hole diameters ranging from 200 nm to 350 nm was fabricated through a free-standing structure made of layers of SiO_2, Si_3N_4, and Au. The growth of antibody immobilized *E. coli* on the gold surface of free-standing structures was monitored using extraordinary optical transmission (EOT). The bacterial growth in the presence of ampicillin and tetracycline changes the refractive index of free-standing structures resulting in shift of EOT peak. Though SPR based AST techniques are rapid and consume a small quantity of analytes (down to single cell), the system is costly, bulky and complex.

3.7. Optical path difference

In another case, Leonard et al. developed a biofunctionalized closely spaced silicon micropillar array platform as a phase grating to study AST (Leonard et al., 2017). These pillar arrays provided a platform to colonize bacterial cells and act as an optical transducing element when optical phase-shift is measured with the help of reflectometric interference spectroscopy as shown in Fig. 2 (II). Periodic Si micropillars were functionalized with Wheat Germ Agglutinin (WGA) to bind bacteria. The optical path difference (OPD) between reflected light from the top surface of the pillar array and the bottom surface was measured. The OPD was strongly dependent on the refractive index of liquid-filled medium and height of pillar. Post-colonization of bacteria, the refractive index of the medium changes and this was measured as a change in OPD. The refractive index decreases when antibiotic above MIC was used as it inhibits the colonization, while untreated colonization over time increases the refractive index. This AST method provided result in less than 3 h in real-time and can also provide MIC.

3.8. Photoluminescence

In another optical detection approach, Nazemi et al. developed an innovative AST based on Photoluminescence (PL) emission of photocorroded GaAs/AlGaAs quantum well (QW) (Nazemi et al., 2017). The QW was formed by depositing 30 pairs of 6 nm thick GaAs and 10 nm thick $Al_{0.35}Ga_{0.65}$ layers sequentially on a semi-insulating GaAs substrate. The QW biochip was functionalized and kept in a bacterial

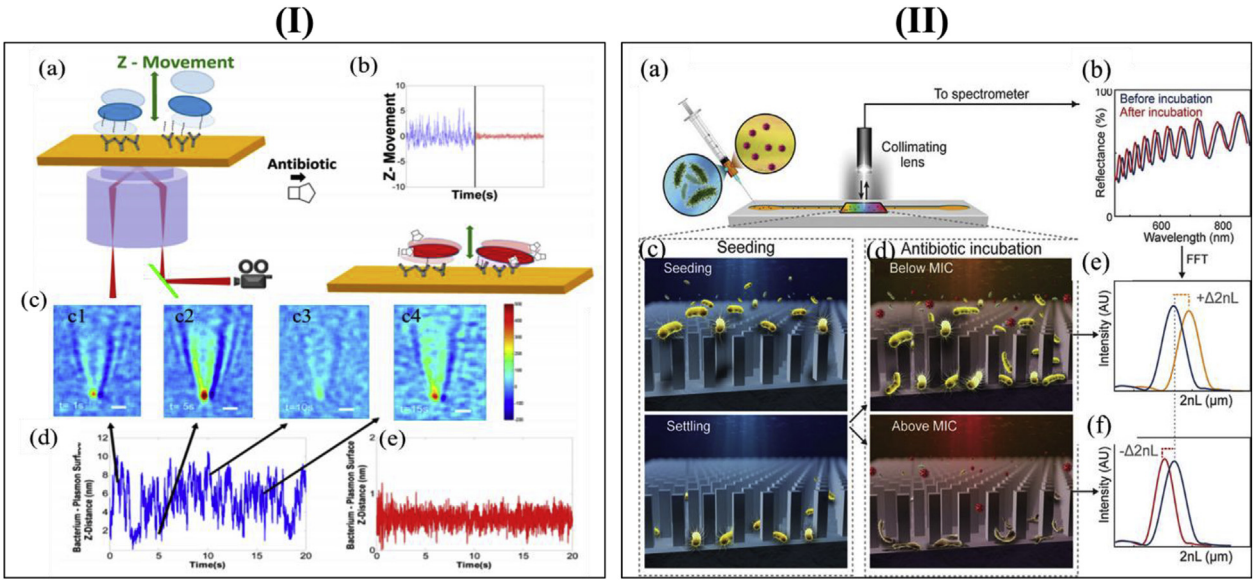

Fig. 2. (I). (a) Schematic setup of plasmonic imaging and tracking of bacterial cells. Surface plasmons were formed when p-polarized light is subjected to gold coated glass sensor chip and reflected light is detected using CCD, (b) Bacterial cell's movement with and without antibiotic treatment, (c) Image of bacterial movement with respect to varying plasmonic image contrast. (d) The plot showing the vertical distance between the plasmon surface and live bacterial cell. (e)The plot showing the vertical distance between the plasmon surface and dead bacterial cell. Reprinted with permission from (Syal et al., 2016). Copyright (2015) American Chemical Society. Fig. 2(II). (a) Schematic representation of phase-shift reflectometric interference spectroscopy AST using photonic chip of pillar-type gratings, (b) Typical reflectance spectra from the grating collected by a spectrometer, (c) seeding stage: bacterial suspension was allowed to settle inside Si pillar chip, (d) Schematic representation of biochip below and above MIC values, (e) Schematic representation of increase in refractive index below MIC, (f) Schematic representation of decrease in refractive index above MIC. Reprinted with permission from (Leonard et al., 2017). Copyright (2017) American Chemical Society.

suspension flow cell so that the electrostatic interaction of bacterial cells with the biochip surface can be monitored by analyzing the intensity and maxima of the PL spectrum. Under the influence of antibiotics, the electrostatic interaction was observed to be decreasing (owing to bacterial death). This caused changes in the PL maxima position over time. This method could provide AST results in less than 3 h for two strains of *E. coli*. However, it used a complex and expensive components and results of the evaluation with other bacterial species have not been reported.

3.9. Bead-based AST

A group of researchers at the University of Michigan, have worked on asynchronous magnetic bead rotation (AMBR) sensor to measure the growth and drug susceptibility of individual bacterial cells (Kinnunen et al., 2012, 2011; Sinn et al., 2012, 2011). In their sensors, magnetic beads were introduced in bacterial suspension and placed within an external rotating magnetic field to control the rotation of the beads. Over time the bacterial cells attach to the beads forming bead-bacteria complexes. The changes in shape, volume, magnetic moment, and environment (viscosity) of the bead-bacteria complex was measured by considering the rotational frequency. In 2011, Kinnunen et al. used a single ball-shaped magnet upon which a single *E. coli* bacterial cell can be attached when the magnet is functionalized with anti-*E. coli* (Kinnunen et al., 2011). During the growth of attached bacteria, the cell length changes due to cell division which leads to change in rotational dynamics. The affected growth dynamics creates a unique detectable signature in the rotational dynamics after addition of antibiotics. By measuring these torque variations, change in length of bacteria as low as 80 nm was sensed. In the improvement of this technique, they had used a self-assembled clustered magnetic microparticles to detect streptomycin and gentamicin MIC against *E.coli* (Kinnunen et al., 2012). This method was rapid (1.5 h) as small changes in bacterial growth was clearly measurable over such a small timeframe. However, this process requires delicately suspended cultures and was not effective for higher concentrations of bacteria. To solve this problem, a novel 48-sensor prototype using standard microwell plates stacked between an aligned light source and photodiodes was used (Kinnunen et al., 2014). In this case, the rotational frequency was temporally tuned to observe the growth of a wide spectrum of bacterial concentrations ranging from 10^8 to 5×10^3 CFU/mL AST of *S. aureus*. In the AMBR sensor discussed above, particle-to-surface stiction effects affect the efficiency and sensitivity of the system leading to limited time for reproducing the results. To alleviate this shortcoming Sinn et al. have used a water-in-oil droplet microfluidics-based AMBR sensor to rapidly measure bacterial growth, susceptibility, and MIC as shown in Fig. 3 (Sinn et al., 2011). In this device, individual AMBR sensors were enclosed in the microfluidic droplets and growth of the individual as well as small bacterial populations was monitored. In 2012, the same group developed a similar droplet microfluidics platform using AMBR sensor-based viscometer to measure AST. The change in the metabolism, motility, and concentration of bacteria changes the viscosity of the medium, which is leveraged (Sinn et al., 2012). These studies are limited to *E. coli* and thus, more studies are needed to be performed to make it more reliable for rapid AST in clinics.

In another study, Chung et al. used carboxylate-/amine-modified polystyrene particles and optical diffusometry principle to quantify the Brownian motion of particles (Chung et al., 2016). The Brownian motion of particles was recorded using a high-speed camera at 10 Hz frame rate for each measurement. When live bacteria (*P. aeruginosa*) are attached to the surface of particles, they move more vigorously due to gaining additional energy from bacteria. However, dead bacteria cause more dragging and thus diffusivity decreases. In this AST method, the temporal diffusivity of the particles is analyzed and it showed excellent results for *P. aeruginosa* against gentamicin within 2 h. Recently, Sabhachandani et al. have used bead-based biosensors combined with droplet microfluidic for capturing and AST monitoring of *E. coli* (Sabhachandani et al., 2017). In this case, *E. coli* suspension and antimicrobial agent are encapsulated in droplet form by using droplet microfluidics (MFD). In the encapsulated droplet, *E. coli* from the patient's sample were easily captured by beads conjugated with antibody. Both antibiotic-induced bacterial growth and phenotype filament formations was studied via fluorescence imaging. This technique had the capability to detect a single cell and produce AST results in 30 min. All these beads assisted methods have a low throughput in screening for an antibiotic or bacteria (in the case of detection) and are limited by an inability to be multiplexed for different assays. He et al. integrated an immunomicrobead-based microfluidic platform for bacterial detection and AST (He et al., 2014). In this study, four PDMS microfluidic units (one for identification and three for AST with different antibiotics) with common output were fabricated on a single chip. In one-unit, bacterial suspension mixed with antibody-coated microbeads were examined using via fluorescence imaging for identification. Remaining three MFD made of linear concentration gradient generator was used for AST. This device could identify bacteria (*E. coli*) in the range of 10^1–10^5 CFU/μL in 30 minutes and provide AST results in 4 h.

3.10. Nanomechanical sensor

In the field of phenotypic AST, nanomechanical sensor-based AST has been an emerging approach in the last decade. A nanomechanical sensor is an ultrasensitive oscillator (cantilevers in most cases) which measures the change in mass induced by the adsorption or selective chemical binding of specific target substance onto the substrate or specimen under study. Atomic Force Microscopy (AFM) based cantilevers are a versatile tool for biochemical sensing applications because of its operational capabilities in different environments such as gases, liquids, or even in vacuum (Lang and Gerber, 2008). It is well known that drugs induce changes in the morphology of bacterial cells i.e. depending on the concentration of antibiotics, varying effects from the creation of pores to complete lysis of the cell wall. The change in morphology of susceptible cells due to antibiotic treatment has been successfully measured using AFM tip by several researchers (Du et al., 2008; Eaton et al., 2008; Fernandes et al., 2009). However, this technique has several limitations such as the complexity of sample preparation, the requirement of an AFM expert to perform the study, the complexity of data interpretation, and an amount of time consumed (Longo and Kasas, 2014). Additionally, it does not provide real-time AST results. To overcome these problems, Longo et al. have developed a microcantilever coupled with an AFM tip to study the micro-motions of cells (Aghayee et al., 2013; Longo et al., 2013). Bacterial cells were attached to the surface of the cantilever and its dynamic fluctuations were measured as a function of time. Nanometer-scale motions of *E. coli*, and *S. aureus* bacteria and their metabolic activities in the presence of antibiotics was studied by measuring the amplitude of fluctuations. A schematic representation of bacteria detection and AST profiling is shown in Fig. 4(I)(Longo et al., 2013). This work was further extended by Lissandrello et al. to measure the nature of force applied by bacterial cells on the microcantilever (Lissandrello et al., 2014). It was observed that the amplitude of the fluctuations strongly depends on the oscillation frequency as well as the number of bacterial cells attached to the surface of the cantilever. Also, the nanoscale motions of prokaryotic and eukaryotic cells and their viability (at a metabolic level) were detected using this technique (Kasas et al., 2015). Thus, it is a promising technology to study and characterize the real-time interactions of bacterial cells with antibiotics. Recently, Johnson et al. studied bacterial vibrations by placing them on a resonant crystal (France et al., 2016; Johnson et al., 2017). In this case, bacterial-induced phase noise i.e. perturbations of resonant crystal boundary conditions and resonant frequency was measured over time to study AST. On exposure of polymyxin B and ampicillin to *E. coli*, the change in phase noise was observed in 7 and 15 min respectively.

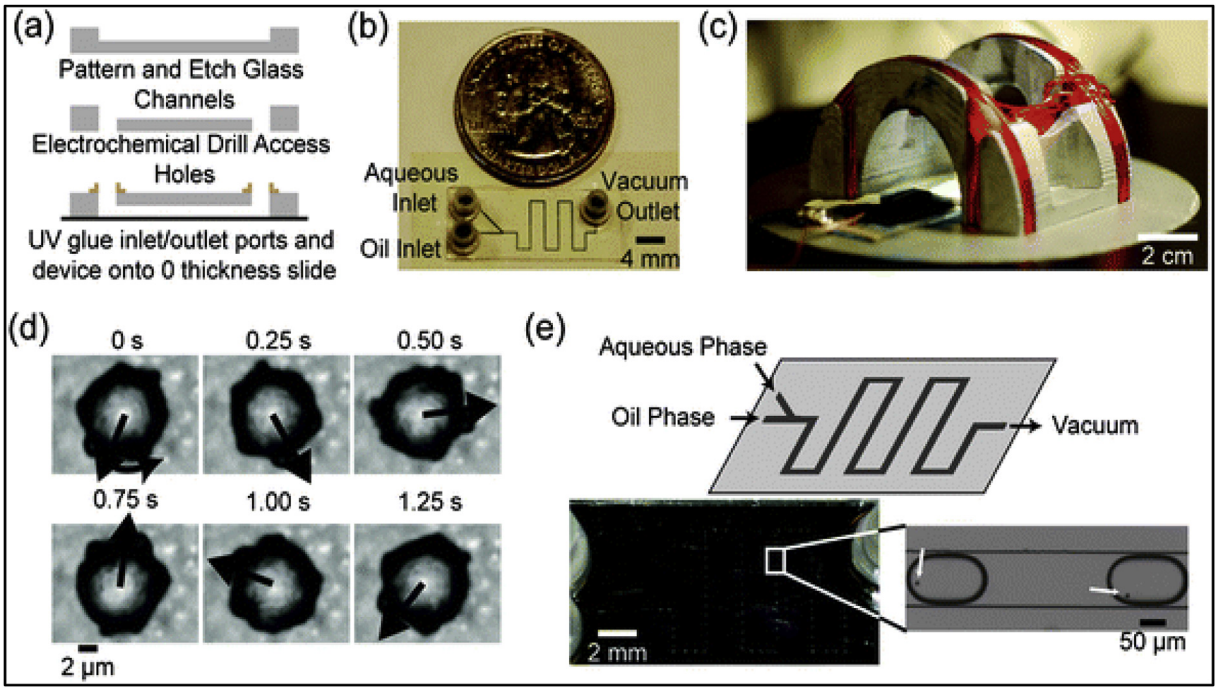

Fig. 3. (a) Schematic representation of microfluidic channel fabrication using standard lithography process, (b) Image of the microfluidic device, (c) An image of the microfluidic device placed inside the electromagnet to generate rotating magnetic field, (d) Magnified image of magnetic bead rotating in an external rotating magnetic field, (e) Image of droplet formation containing magnetic beads. Reprinted with permission from (Sinn et al., 2011). Copyright (2011) The Royal Society of Chemistry.

Another efficient mechanical sensing method is based on quartz crystal microbalance (QCM). In 2015, Ma et al. utilized electrochemical QCM-based lectin biosensor for AST profiling (Ma et al., 2015). Antibiotics induce changes in the carbohydrate and lectin adhesin structures of bacterial cell walls, which leads to alterations of lipopolysaccharide (LPS) chain lengths and lectin expressions. Thus, the binding strength of bacteria cells on QCM surface via LPS was crippled. The effect of ciprofloxacin, ceftriaxone, and tetracycline on *E. coli* suspension showed at least 10% change in resonant frequency after 1 h.

3.11. Opto-mechanical techniques

In another approach, buoyant mass and instantaneous growth rates of individual bacterial cells were measured with the help of MFD embedded on resonant cantilever (Gfeller et al., 2005; Godin et al., 2010; Knudsen et al., 2009). The position of individual bacterial cells in an MFD was determined by measuring the changes in the resonant frequency. This method could detect different bacterial cells and their changes in volume, mass, and density. The difference between antibiotic-resistant and antibiotic-susceptible bacteria was also verified. A similar approach was developed by Etayash et al. for AST measurement by integrating photothermal infrared spectroscopy with a bi-material microchannel cantilever (Etayash et al., 2016). This device was designed to measure the adsorbed mass, adsorption stress, and mid-infrared spectroscopy of the adsorbates (in this case, bacterial cells) which improved the sensitivity and selectivity. This scheme is shown in Fig. 4(II). In this case, antibodies captured specific bacteria cells on the cantilever. These immobilized bacterial cells upon absorption of heat from specific frequency ranges of the incident IR light caused changes in the resonant frequency of the cantilever. The live and antibiotic-induced dead bacteria was studied by measuring changes in the oscillation frequency of the cantilever. These nanomechanical sensors for AST application are rapid as compared to other methods. However, it requires a pure isolated bacterial culture and may not be useful for mixed bacterial population or non-bacterial cells. Implementing multiplexing to provide AST results for multiple antibiotics is also challenging. In this regards, Kara et al. had used fine MFD filled with PBS solution to monitor ultra-movement of bacteria via measuring electrical resistance through the channel (Kara et al., 2018). When bacteria cells were present inside the fine microfluidic channel, the effective diameter of the channel was reduced resulting in a voltage drop due to resistance faced by ions. These small voltage fluctuations were recorded with the help of lock-in-amplifiers over a period of time to measure the effects of the antibiotic on the *E. coli*. Though this method is simple, rapid, and requires small to no sample preparation, it will be not useful for non-motile bacteria (e.g. *S. aureus*). In another study, resonator frequencies depend AST was carried out by placing multiple mass sensors in a suspended microfluidic channel (Cermak et al., 2016). Here, these resonant mass sensors were placed along the channel but separated by 'delay: to give sufficient time to grow' to measure growth rate i.e. increased mass in the successive sensor. This serial suspended microfluidic resonator was tested for various cells including *Saccharomyces cerevisiae, E. coli, and E. faecalis* bacteria cells. For AST profiling, the normal and bacterial suspension mixed with antibiotics was made to flow through the channel and their growth was measured at 0.02 pg/h resolution.

3.12. Microfluidics technologies

In microfluidics technology, an extremely small amount of fluid can be accommodated and manipulated to yield interesting biophysiochemical changes and effects (Whitesides, 2006). The size of these devices can vary from the nanometer to centimeter scales. With the help of advanced nanotechnology and microfabrication techniques, researchers have fabricated miniaturized chambers (micro-liter to pico-liter), channels as well as other structures like porous membranes, slits, etc. (Leester-Schädel et al., 2016; Whitesides, 2006). Polydimethylsiloxane (PDMS), glass, silicon, silicone elastomer, or plastic are the most preferred material in microfluidics device fabrication. In biological applications, the prime utility of 'lab-on-chip' platform is to

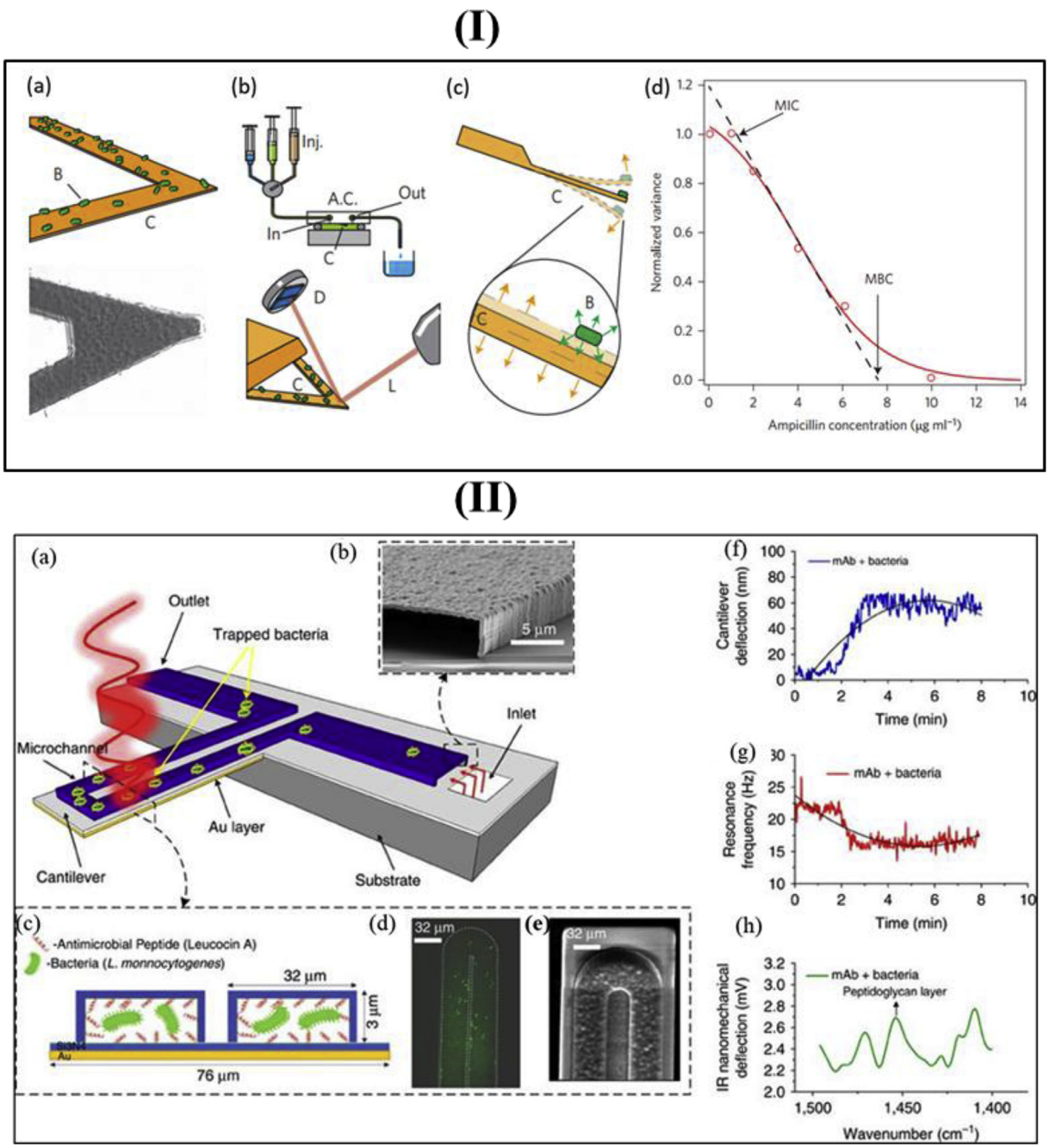

Fig. 4. (I) (a) Schematic and SEM image of cantilever functionalized with bacteria, (b) In an optical image (bottom), several attached bacteria can be visualized, (b) Schematic representation of acquisition chamber (A.C.) with help from laser beam, L and detector, D, (c) Schematic representation of cantilever fluctuations during bacterial presence, (d) Bacterial presence fluctuations measured in presence of antibiotics. Reprinted with permission from (Longo et al., 2013). Copyright (2013) Nature Publishing Group Fig. 4(II) (a) Schematic representation of microfluidic channel on a bi-material cantilever (BMC) for AST application, (b) Cross-sectional Scanning Electron Microscopy (SEM) image of microfluidic channel, (c) Cross-sectional schematic of the microfluidic channel filled with bacterial suspension and antibiotics, (d) Green fluorescent image of microfluidic channel filled with bacterial suspension, (e) SEM image of microfluidic channel tip, Time evolution of (f) cantilever deflection, (g) Resonance frequency of cantilever beam, as more and more bacteria gets immobilized on the cantilever using mAb, and (h) Frequency range over which bacteria absorbs IR light detected through nanomechanical deflection. Reprinted under creative commons licence from (Etayash et al., 2016) Nature Publishing Group.

create a controlled physical or chemical environment via geometric manipulations with the capability to manipulate liquids and study the changes in the biochemical behaviour. Diverse microfluidic architectures have been used for different applications such as gradient generation, droplet-formation, microchamber array formation, etc. The changes in physical or chemical behaviour of biological samples in microfluidics were monitored through various modalities such as optical, magnetic, and electrical. Overall, these lab-on-chip platforms have several advantages like allowing for multifunctional implementation (e.g. amplification, cell lysis, and hybridization), ensuring high sensitivity, reducing the workload, and making the testing less expensive.

In the last twenty years, several researchers have studied bacterial culture using microfluidics and have found that bacterial division in small volume is faster, which may potentially reduce AST time. Connell et al. showed that bacterial behavior was strongly dependent on the

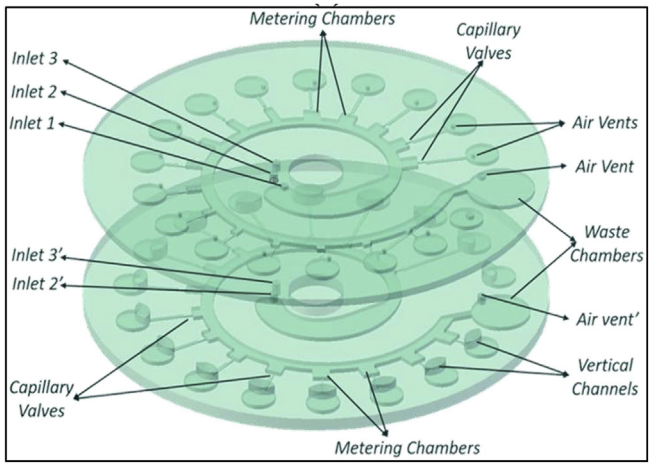

Fig. 5. Schematic of the two-layer disc for gradient generation. Gradient of antibiotic was generated by rotating the disc. Reprinted with permission from (Tang et al., 2018). Copyright (2018) The Royal Society of Chemistry.

geometry of microfluidics (Connell et al., 2013). In 2010, Chen et al. demonstrated that growth of bacterial cell strongly depends on the volume of the culture medium (Chen et al., 2010). They proved that the enhanced surface area-to-volume ratio of growth chamber like in microfluidics increases the growth rate of cells. Researchers are interested in single bacterial cell separation and its AST behavior over time. For this, several techniques such as droplet microfluidics, microchambers, bacterial capturing and their confinement, bacterial traps, and channels/tracks have been developed (Choi et al., 2014, 2013; Dai et al., 2013; Long et al., 2013; Lu et al., 2013; Peitz and van Leeuwen, 2010; Rowat et al., 2009; Sinn et al., 2011). Baltekin et al. used a narrow microfluidic trap to study AST and were able to provide results in less than 30 min (Baltekin et al., 2017). The growth of trapped *E. coli* in the presence of antibiotics was studied using automated phase contrast microscopy and post image processing.

With emerging engineering technologies, there is a wealth of work dealing with microfluidic for AST applications as reviewed by Campbell et al. and Dai et al. (Campbell et al., 2016; Dai et al., 2016). One such study is a multiplexed microfluidics device developed by Mohan et al. for AST application (Mohan et al., 2013). In this work, an array (4 × 6)-of microwells, with each microwell straddled by fluid lines on either side for loading antibiotics and bacterial suspension was fabricated for the study of bacteria-antibiotic interaction. The effects of an individual as well as multiple antibiotics with variable concentrations were studied on *E. coli*. This multiplexed microfluidics device provided AST results in less than 4 h and the total volume of reagents used for this test was ~6 µl. In their next work, a similar kind of multiplexed microfluidic device was used for polymicrobial suspension (Mohan et al., 2015). In majority cases in the literature, AST has been reported to be performed on monomicrobial cultures whereas polymicrobial AST is complicated due to inadequate antimicrobial dosing regimen of different bacteria. This device had 48 wells for diffusion mixing and, half the part of each microwell was covered by polymicrobial suspension and the other half by antimicrobial solutions. The analysis of the kill curve after 16 h of incubation provided information about AST results. In another study, Dai et al. have worked on multiplexed nanoliter reactors (1 nL) that allows for different cell cultures in parallel (Dai et al., 2013). The device was designed in such a way that flow channels and culture reactors will maintain uniform bacteria numbers in variable environments in a single run. This device was integrated with a fluorescence imaging system to study bacterial growth in the presence of various concentrations of antibiotics. Recently, Matsumoto et al. have used four channel based microfluidics device with one shared inlet for AST application (Matsumoto et al., 2016). This device allows for testing against three different concentrations of antibiotics against *P. aeruginosa*. AST was microscopically evaluated by counting cell numbers and morphological observation.

3.13. Gradient microfluidics

In a 96-well plate, a concentration gradient antibiotic can be generated and tested against bacteria. However, this process is laborious and consumes large volumes of reagents. With the help of microfluidic engineering technology, some research groups have developed on-chip gradient generator (Hou et al., 2014a; Li et al., 2014). These gradient generators were formed in discrete or continuous versions with the help of different channel configurations, microfluidic traps, or hydrogel slabs. Kim et al. have fabricated a fivefold gradient generator to monitor biofilm disruption under the influence of several antibiotics (Pil Kim et al., 2010). Similarly, Hou et al. have used a commercially-available microfluidic device having a 6 µL chamber to test a range of antibiotic concentrations against *E. coli*, *S. aureus,* and *Salmonella Typhimurium* (Hou et al., 2014b). The bacterial response over a linear concentration gradient of antibiotics was observed using a phase contrast microscope to determine growth over time and against various concentrations to obtain the MIC value. A similar approach analogous to classical E-test was used to determine MIC corresponding to an optimal bacterial concentration (Malmberg et al., 2016). Recently, Tang et al. developed an automated linear concentration gradient generator based on centrifugal microfluidics for AST applications (Tang et al., 2018). This device consists of a multilayer microfluidics platform in the shape of stacked discs where the individual layer was fed with DI water (layer-1), ampicillin (layer-2) and *E. coli* suspension (layer-3) as shown in Fig. 5. After spinning the disc at various speed, 16 linear gradient antibiotic concentrations were generated in the metering chamber and they were further mixed with an equal amount of *E. coli* suspension after passing through capillary valves. Once each fluid reaches the mixing chamber, the disc was incubated, and absorbance of each chamber was measured sequentially. This device provided AST results in 3 h. Kim et al. have developed a miniaturized broth microdilution platform based on concentration gradient microfluidics for AST application(Kim et al., 2015). In this study, pressure driven microfluidics was used to generate different concentrations of antibiotic which were mixed with bacterial culture (5×10^5 CFU/mL) in 30-nL chambers. Bacterial behaviour was monitored using standard phase contrast microscopy over time to determine the effect of antibiotics. In another study, Derzsi et al. developed a gradient microfluidic based on geometry controlled hydrodynamic traps that passively meter, merge, route, and retain nanoliter samples via capillary action (Derzsi et al., 2016). This device was operated through five pipetting steps, three for loading the aqueous samples namely bacterial culture, antibiotic and pure broth as a diluent and two steps for maintaining the flow in the device. The metering requirements in the device are for creating equal volumes of bacterial culture using pure broth and concentration gradients of the antibiotics. The metering as well as the flow in the chip creates the required droplets for analysis. This chip gave a dilution ratio of 1.68 (although it was designed for 2) in 11-fold. It was successfully tested with *E. coli* strain against ampicillin and provided AST results in 4 h after pipette loading.

In most cases, microfluidic chips are operated by means of pumps. On the other hand, Ran et al. have developed a pump-free micro-device for AST analysis (Ran et al., 2015). In this study, a circular well (5 mm in diameter) and a V-shaped microfluidic channel (200 µm wide and 1000 µm length on each side) were fabricated in such a way that the intersecting portion of the V-shaped channels would terminate by just touching the well wall. The channel and the well wall were separated from each other by a set of parallel micropillars as a diffusion barrier. Upon loading antibiotic in the well, they start diffusing towards the channels which were loaded with bacteria mixed agarose gel. The antibiotic diffuses from the well towards the channels and as a result, a

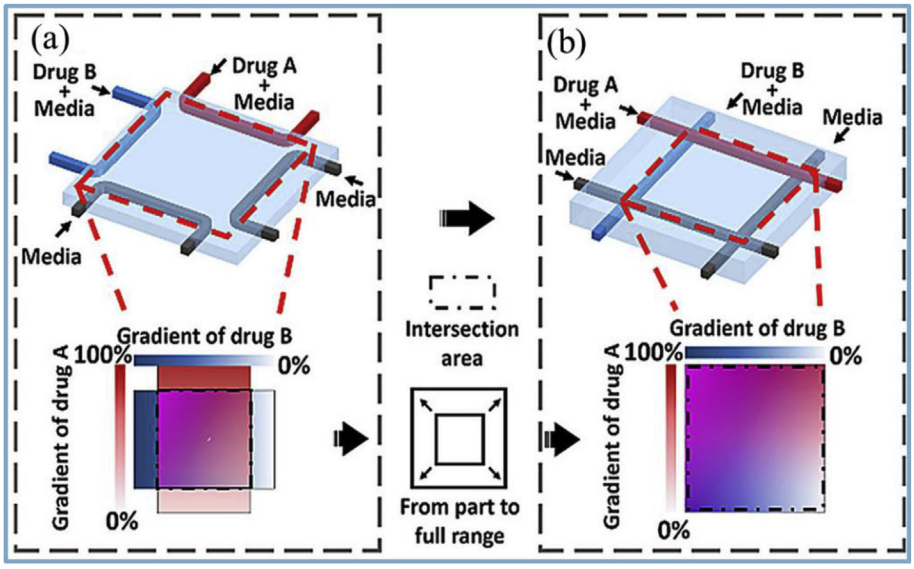

Fig. 6. Schematic of two-dimensional linear gradient AST: (a) Design to generate gradients with two different drugs. This device can't use full range of antibiotics, (b) Modified design to generate full range (0–100%) of antibiotics gradients. This design enables to use multiple number of antibiotics and their corresponding gradients. Reprinted with permission from (Liu et al., 2017). Copyright (2017) Wiley Online Library.

concentration gradient is generated along the channels. The bacterial behavior in the presence of gradient antibiotic concentration was studied using fluorescence imaging. Though this method was simple and was able to perform AST within 4 h it was limited by the requirement for large amounts of reagents. The gradient profiling is time dependent and thus one has to wait till the diffusion process completes to start the testing.

Instead of conventional microfluidics, Sun et al. have developed hydrogel microfluidics by combining conventional plate culture to study AST (Sun et al., 2016). A liquid mix of agar and sodium alginate gel was cast on PDMS mold to solidify after which solid gel slices were bonded with help of $CaCl_2$ solution. To generate a linear gradient of antibiotics across the square shaped solid porous gel, four channels were designed to surround this zone from four sides to flow antibiotics and LB broth as shown in Fig. 6(a). Bacteria were cultured on above this square region and their interaction with antibiotics were monitored via fluorescence imaging. This device was capable of testing against two gradients and the same group went on to improve this technique to test with multiple antibiotics across a range of concentrations (Liu et al., 2017). However, this design restricted the generation of complete concentration gradient range of 0–100%. In their improvised version, three layers of solid gel slices were bonded so that channels can bypass each other as shown in Fig. 6(b). By designing parallel channels in one layer and orthogonal parallel channels in another layer, several square zones were formed. This device was able to generate multiple gradient zones of individual or combination of antibiotics and also allowing for the entire concentration range of 0–100% to be covered which was a limitation in the previous design. The test results of *E. coli* against ampicillin, gentamicin and their combination were produced in less than 5 h. However, the durability of this device was not tested and thus, more studies are needed.

3.14. Droplet microfluidics in AST

In droplet microfluidics, droplets are formed either by continuous flow of the emulsion or by electrowetting. In AST applications, bacterial cells and the antibiotics to be tested against were encapsulated in the form of droplets in a favourable cellular environment (Kaminski et al., 2016). In 2008, Boedicker et al. used droplet microfluidics to accelerate *S. aureus* growth and measure AST against different antibiotics (Q. Boedicker et al., 2008). This device provided results after 7 h of incubation and was limited only by the formation and measurement of droplet volume. This device was also capable of delineating methicillin sensitive and resistant strains of *S. aureus* from human blood plasma. In this case, separate devices were used for droplet generation, droplet incubation, and droplet detection. To reduce AST time, Kaushik et al. developed a droplet-based fluorescent AST device with inbuilt incubation zone as shown in Fig. 7. (Kaushik et al., 2017). This device provides AST results in 1 h and is one of the fastest phenotypic AST devices. Similarly, Baraban et al. used a novel millifluidic droplet analyzer (MDA) to determine the growth rate of E.coli and calculate its MIC against specific antibiotics (Baraban et al., 2011). Digital screening of multiple antibiotics or combined antibiotics on *E. coli* using an automated microfluidic platform was carried out by Churski et al. (2012). In this case, resazurin (a fluorescent dye) was used to track bacterial behaviour and AST was performed within 3 h. This device was programmed for automatic droplet formation and sequential detection using optical imaging. The major advantages of droplet microfluidics were the ability to fine-tune droplet size, bacterial density, antibiotic concentrations, and reproducibility. In 2006, Jiang et al. demonstrated a unique droplet-based millifluidic technique to study AST accurately (Jiang et al., 2016). This millifludic system was analyzed with a MilliDrop Analyzer and results were in good agreement with classical as well as VITEK®2 technologies. However, droplet microfluidics has not yet been tested with multiple bacteria or combinations of bacteria with different antibiotics and thus, more studies need to be carried out in this field.

3.15. Stress-induced AST

By applying mechanical stress and antibiotics, Kalashnikov et al. have developed a microfluidics AST technique to accelerate the death of susceptible strains (shown in Fig. 8) (Kalashnikov et al., 2018, 2017, 2014, 2012). Bacterial cells were immobilized on the channel floor by epoxy coating to hold them in place under high flow rates. Mechanical and enzymatic stress was applied on these immobilized bacteria by flowing growth media containing Sytox green, which is a fluorescent stain confirming the loss of cell viability. An enzyme Lysostaphin that cleaves linkages in the bacterial cell wall, bacterial culture media, and antibiotics at high speed by inducing enzymatic stress. The antibiotics inhibit the cell wall repair pathways that get triggered by the stress-inducing enzyme. The effect of antibiotics was examined via phase contrast and fluorescence microscopy through visualization of the Sytox Green dye. This stress-induced AST could distinguish between methicillin-resistant *S. aureus* and methicillin-sensitive *S. aureus* in less than 30 min (Kalashnikov et al., 2014, 2012). In their next work, they

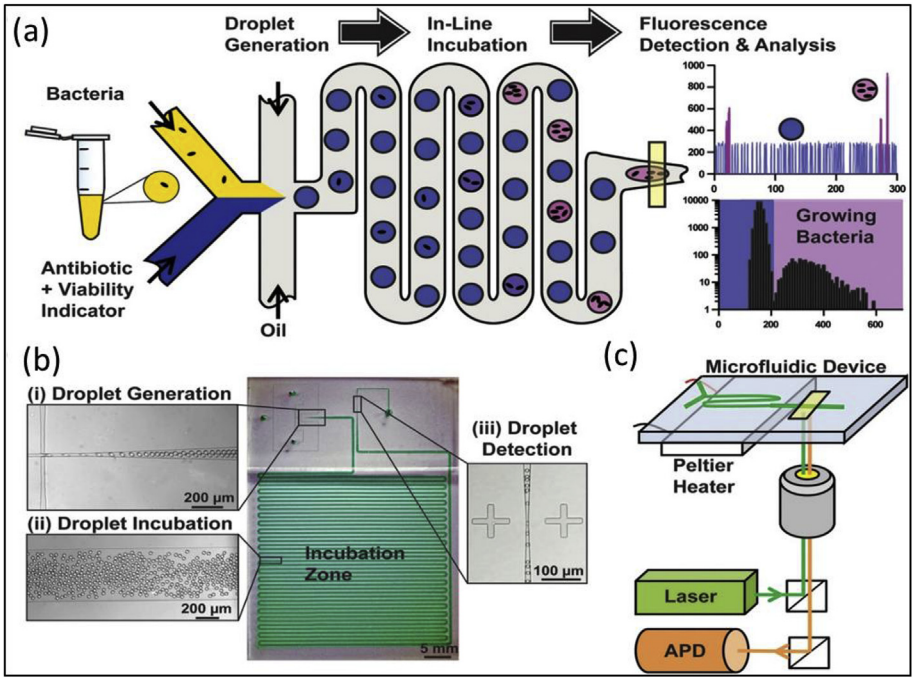

Fig. 7. (a) Schematic representation of droplet formations embedded of single bacteria cell and antibiotics. These encapsulated droplets are incubated (by keeping them in an incubation zone) for bacteria growth and study droplets were analyzed using fluorescence imaging, (b) Image of droplet generation during continuous flow, (c) Schematic representation of the droplet analysis by fluorescence imaging using a laser excitation source and an avalanche photodiode detector. Reprinted with permission from (Kaushik et al., 2017). Copyright (2017) Elsevier.

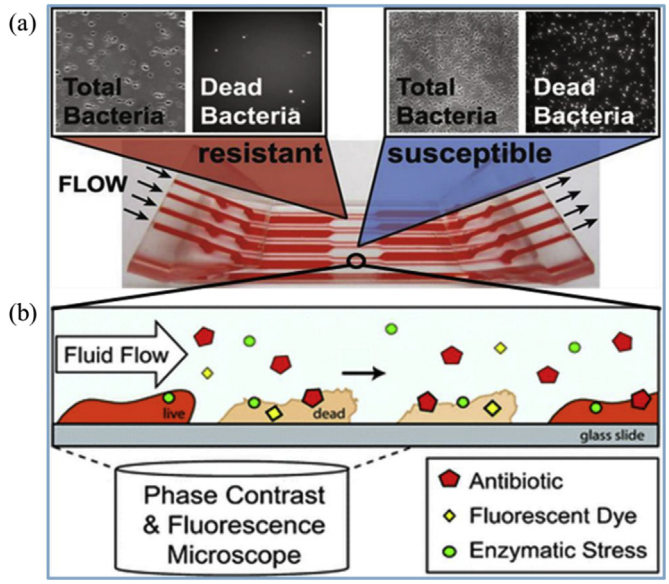

Fig. 8. (a–b) Stress induced AST using microfluidics device. Cross-sectional view of a single microfluidic channel AST action. Bacterial behavior was monitored using phase contrast and fluorescence microscope. Reprinted under creative commons licence (Kalashnikov et al., 2017) Nature Publishing Group and reprinted with permission from (Kalashnikov et al., 2012) Copyright (2012) The Royal Society of Chemistry.

successfully tested against several gram-negative bacteria namely, *Enterobacter cloacae, E. coli, Klebsiella pneumoniae, Pseudomonas aeruginosa* and gram-positive bacteria *S. aureus*(Kalashnikov et al., 2017). Most recently as a next step, the temperature, mechanical stress, chemical stress, and media compositions were varied to optimize the AST performance (Kalashnikov et al., 2018). Despite uniqueness and robustness of this measurement modality, there are several concerns that needs to be addressed: such as requirement of large volumes of reagents, possibilities of leakage owing to high flow rate of liquid in the channels and change in morphology of resistant bacteria after the experiment which could be considered as a collateral damage of the experiment itself.

3.16. Microchamber-based AST

In droplet microfluidics, droplets are motile and thus, manipulating, handling, and tracking them is relatively complex. Recently, few researchers have reported the development of microchamber (static) based AST. In 2014, Weibull et al. fabricated nanoliter wells (336 wells per device) which offers simple loading, multiplexing, and imaging for AST applications (Weibull et al., 2014). The growth of *E. coli* in nanoliter chamber against ciprofloxacin, cefotaxime, and ampicillin was observed in real-time using optical density measurements. They have developed a mathematical algorithm to calculate the lag phase of bacterial growth which allowed for determining MIC within 4 h. Considering the design and structure of these microwells, it was difficult for these wells to be completely isolated from each other during the testing process, thereby casting apprehensions on the utility of this platform to be used for multiplexing. Recently, Avesar et al. have developed chemically isolated nanoliter wells (8 nL) for rapid AST (Avesar et al., 2017). Here, the multiplexing was carried out by creating rows of nanowells with a common delivery channel. The mixed bacterial culture with antibiotics was used to fill the wells via a common delivery channel. The wells were chemically isolated by flowing oil through the same delivery path as shown in Fig. 9. Further, the biochemical activity of the bacterial cells within each well was monitored using conventional fluorescence imaging. Also, an algorithm was developed for the automated analysis of susceptible/resistant strains. In another study, eight individual microchambers (volume-360nL) with two flow channels were fabricated to determine the MIC for microbes (Takagi et al., 2013). Channel 1 was used to load bacterial suspension and channel 2 was used for suction of suspension into the chamber. Prior to making the device via bonding of PDMS with the glass substrate, antibiotics solution with 0/5 wt% BSA was loaded onto the PDMS chambers and freeze-dried to form a matrix. Variable concentrations of different freeze-dried matrices were used to study the growth of *E. coli*.

3.17. Agarose based cell tracking

In most cases, cells in MFD are in constant motion and thus tracking of individual cells is a difficult task. Also, shear flow affects the morphology of cells. Few research groups have alternately used agarose in

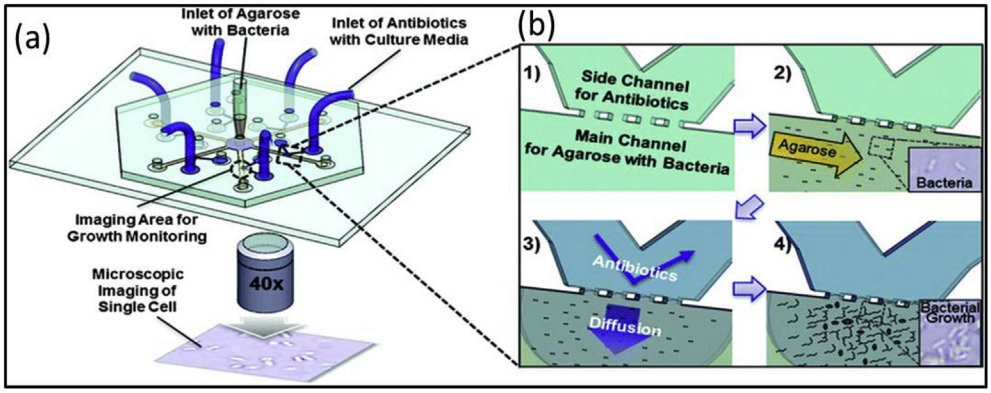

Fig. 9. (a) Schematic representation of multiplexed microfluidic agarose channel for AST. This device is loaded with agarose–bacteria mixture in centered inlet and antibiotics at periphery inlet, (b) (1) Channel without any loading, (2) agarose–bacteria mixture loading, (3) Antibiotic loading. Here diffusion of antibiotics happens through capillary valve, (4) Bacterial behavior is recorded using a microscope and a time lapse method. Reprinted with permission from (Choi et al., 2013) Copyright (2013) The Royal Society of Chemistry.

MFD to freeze individual cells and study their AST profiles. Choi et al. have worked on microfluidic agarose channel based systems for tracking single bacterial cells and applied for rapid AST studies (Choi et al., 2014, 2013). In their first system, liquid agarose with bacteria and culture media containing antibiotics was flown in two channels separated by a capillary valve (shown in Fig. 9) (Choi et al., 2013). In the next step, bacteria cells were immobilized by solidifying the agarose. The culture media containing antibiotic was allowed to diffuse towards the agarose frozen channel. Bacterial growth in the presence of different antibiotics with variable concentration was then monitored for AST. The same group extended this work using microfluidic agarose channel integrated with a 96-well platform i.e. individual well and microfluidics channel were placed side-by-side and separated by a capillary valve (Choi et al., 2014). In this study, the morphology of individual cells was analyzed in the presence of antibiotics with the help of time-lapse microscopy. An algorithm was developed to match with gold standard broth microdilution technique (91.5% agreement). In another study, the same device was used to carry out direct and rapid antimicrobial susceptibility testing (dRAST) of bacterial samples from a positive blood culture bottle and provided AST results (91.11% success) in 6 h. This is of particular interest as most studies are only on clinical isolates (Choi et al., 2017). Recently, the same platform was used to test on *Mycobacterium tuberculosis*. The drug susceptibility test results were obtained in 9 days, whereas conventional drug susceptibility tests for *Mycobacterium tuberculosis* takes around 4–6 weeks (Choi et al., 2016). In 2014, Li et al. worked on a unique AST device having a thin agarose gel membrane coated with a monolayer of bacterial suspension which was sandwiched between glass and PDMS layer (Li et al., 2014). Two parallel PDMS channels (namely source and drain) were allowed to flow amoxicillin and plain medium so that a concentration gradient of amoxicillin formed between the source and drain through agarose. Morphological dynamics of sandwiched bacterial cells under the influence of gradient of amoxicillin were recorded for AST.

3.18. Microfluidic pH sensor

During bacterial growth, the glucose-containing medium becomes more acidic due to the accumulation of organic acids. Based on this idea, Funfak et al. have used pH-dependent fluorescent polymer particles in microfluidic channels to study the metabolic activity of *E. coli* cells (Funfak et al., 2009). In 2013, Tang et al. developed a microfluidic platform to measure changes in pH for AST applications (Tang et al., 2013). In this device, a microfluidic channel was fabricated on the porous silicon surface by integrating pH-sensitive chitosan hydrogel. Bacterial cells were confined in a nanoliter size channel which results in rapid changes in metabolic activity and thus pH changes rapidly. Based on the pH of the medium, the chitosan hydrogel either shrinks or swells and this was recorded with Fourier transform reflective interferometric spectroscopy (FTRIFS) which measure the effective optical thickness (EOT) of chitosan hydrogel as shown in Fig. 10. *E. coli* suspension, cultured in glucose medium, was tested against ciprofloxacin, tetracycline, azithromycin, and amikacin. It was found that the EOT is inversely related to the pH i.e. lower EOT results from bacterial inhibition and higher EOT results from bacterial growth. This device provided AST result within 2 h. However, after Tang et al. no other researcher has explored this technique further.

In general microfluidics devices require valves and actuators to operate. However, Cira et al. developed a portable microfluidic device that has dead-end chambers where bacterial samples were loaded and isolated from others (J. Cira et al., 2012). In this case, a set of PDMS chambers were fabricated and dried antibiotics were stored in them. This PDMS layer containing chambers was bonded with a second PDMS layer having microfluidic channels to connect the chambers. The chambers, as well as the channel, were degassed via vacuum as PDMS is permeable to the flow of gases helping the chambers and channels to be degassed. The bacterial suspension is then sucked into the device during the loading process because of the vacuum inside. In this degassing driven device, the interaction of antibiotics and bacteria in the chamber was visualized with a pH indicator (colorimetric change) i.e. as bacteria grow, they produce organic acids by degrading glucose and thus pH decreases. This is a self-loading device which needs only a few microliters of the bacterial suspension. This AST device was tested with various concentrations of vancomycin, tetracycline, and kanamycin against *Enterococcus faecalis*, *Proteus mirabilisHI4320*, *Klebsiella pneumoniae,* and *E. coli.*

3.19. Dielectrophoresis

Dielectrophoresis is a nonlinear electrokinetic phenomenon in which a force gets exerted on dielectric particles such as bacterial cells when a non-uniform electric field is applied. The particle movement is strongly dependent on the strength of the local electric field, medium, and the permittivity of the particles. Based on this principle, Johari et al. have studied the viability of bacterial cells by applying an electric field of frequency 100–200 kHz (Johari et al., 2003). The movement of the cells towards high and low electric fields was used to differentiate between viable and non-viable cells. Similarly, Braff et al. discriminated bacterial species at the strain level for *P. aeruginosa* and *S. mitis* by immobilizing them with the electric field in a microfluidic channel (Braff et al., 2013). The immobilized bacterial cells images were processed to study bacterial behaviour. Chung et al. have worked on dielectrophoresis-based AST by measuring dielectrophoresis behaviour and elongation rates of *E. coli* (Chung et al., 2011). They designed a quadruple electrode to create a non-uniform electric field as shown in Fig. 11(I) (a-c). Under the influence of β-lactam antibiotics, the crossover frequency (transition frequency as particles moves from high electric field region to low electric field region) of the bacterial suspension and cell elongation was measured. This test provided AST results in less than 2 h. Subsequently, they tested with cephalosporin-resistant *E. coli* and cephalosporin-resistant *K. pneumoniae* against

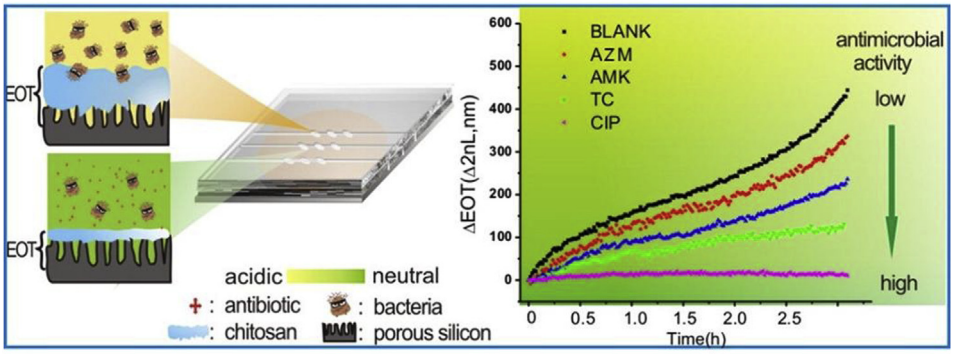

Fig. 10. Schematic representation of microfluidics pH sensor. The effective optical thickness of porous silicon and chitosan hydrogel was measured by considering antibiotics induced pH change. Reprinted with permission from (Tang et al., 2013) Copyright (2013) American Chemical Society.

cefazolin(CEZ) successfully (Chung et al., 2012). According to these results, CEZ treatment caused reduction of cross-over frequency of bacterial suspension to hundreds of kHz and cell length increased more than 10 μm (which is usually the average cell length of healthy cells). This work was further extended to study bacterial behaviour in a resistant and susceptible mode in the presence of different antibiotics with variable concentrations (Su et al., 2017). Cell elongation of antibiotics induced susceptible bacteria, cell swelling, or lysis, as well as the behaviour of resistant bacteria (whether the numbers are unchanged, or they increased), was monitored using this technique Fig. 11(I) (d).

In another approach, electrokinetic AST was used to capture bacterial cells at the edge of microelectrodes by dielectrophoresis method and they were analyzed with an automated image processing to single-cell resolution in the presence of antibiotics (Peitz and van Leeuwen, 2010). In this study, an additional DC field was applied between interdigitated electrodes and a redox reagent was flown in the microfluidic channel to capture and immobilize bacteria on the electrode surface. AST of *E. coli* K12 against Polymyxin B was successfully monitored and determined MIC as well as IC50 values. A similar approach by Lu et al. for AST was carried out by narrowing the channel width to the range of bacterial cell diameter (Lu et al., 2013). In this study, *E. coli* cells were loaded onto the confined microchannels (0.5–10 μm width) by the electrokinetic method and their growth was monitored at the single cell level. The position of the bacterial cells inside the channel was tailored by controlling the electric field and subsequently, the growth rate was observed using phase contrast microscopy. The growth rates with and without ciprofloxacin antibiotic were easily differentiated in less than 1 h. All these dielectrophoresis-based AST studies were performed on few bacterial species and strains and thus, may not be generalized for an exhaustive antibiotic-bacteria combination yet.

3.20. Electrochemical sensing

Electrical biosensing is considered a robust, miniature, label-free, low-cost, rapid, and easy-to-handle technique. These devices are highly sensitive and are considered as the most practical assessment tool for point-of-care diagnosis (Bhalla et al., 2016; Luo and J. Davis, 2013; Mehrotra, 2016; Turner, 2013; Vigneshvar et al., 2016). In most cases, biological targets are made to bind with the target antibody and the perturbations in the current or voltage signal are measured. Several biosensors like amperometric/voltammetric biosensors (current measurement), potentiometric (voltage/charge measurement), conductometric (medium conductance measurement), impedance biosensors (electrical impedance measurement with varying input potential and frequency) and field-effect transistor (FET) biosensors (current or potential measurement across a semiconductor by tuning gate potential) are widely used. Electrical biosensors have been frequently used to detect bacteria and their growth over time. In most amperometric electrochemical systems, ferri-/ferrocyanide is used to monitor bacterial suspension (Chotinantakul et al., 2014; Ertl et al., 2003, 2000; Mann and Mikkelsen, 2008). The measured current in amperometric electrochemical AST strongly depends on Fe(II) oxidation which is proportional to the number of cells available in the suspension. Under the influence of antibiotics above MIC, the current decreases as compared to resistant bacterial suspension or a bacterial suspension with no antibiotics added. Amperometric/voltammetric AST systems are relatively faster than conventional as well as few engineered AST technologies. Besant et al. have studied a phenotypic electrochemical approach for AST applications (Besant et al., 2015). In this case, bacterial cells were captured in confined nanoliter wells integrated with working, counter and reference electrodes. The loaded bacterial cells were cultured with antibiotics and an electrochemically redox-active molecule like resazurin. Resazurin gets reduced actively when live resistant bacterial cells are present in the suspension leading to changes in current profiling. If majority susceptible cells are there the extent of reduction reaction is lesser leading to negligible changes in the current profile. This method provided AST results in one hour and is one of the most efficient and low-cost techniques currently available.

3.21. Impedance spectroscopy

Impedance measurement is one of the simplest techniques used for AST, where an alternating current (AC) signals of a wide range of frequencies are applied to a suspension and its impedance response is measured. Under the influence of AC field, live bacterial cells in suspension act as polarized particles leading to charge build-up across their cell membrane which acts like capacitors. The total capacitance strongly depends on the number of bacteria cells available in the suspension. In most cases, antibiotics above MIC value causes lysis of cells which leads to the increase in conductive species like carbonate and lactate in the suspension as it gets out of the cytoplasm of the cell into the suspension medium. Total resistance, as well as capacitance change of the suspension, is measured to find out the effect of antibiotics. Recently, Jo et al. has performed AST experiment by measuring the changes in capacitance of *E. coli* and *S. aureus* suspension in the presence of gentamicin, ampicillin, and tetracycline (Jo et al., 2018). In this study, an array of interdigitated electrodes (IDE) was fabricated on a glass substrate and each electrode area was confined by acrylic wells. The sensor surface between the electrodes was functionalized by DNA aptamers to immobilize bacterial cells. The frequency dependent capacitance of bacterial suspension with and without antibiotics was measured in real-time. It was found that capacitance of the suspension decreases over time when antibiotics above MIC was added and increases when this concentration was below MIC, indicating bacterial growth over time in the absence of effective antibiotics. In another AST study, 3-aminophenylboronic acid (3-APBA) was used to bind to polysaccharides on the bacterial cell walls to immobilize them and measure the changes in capacitance with and without the antibiotic drug

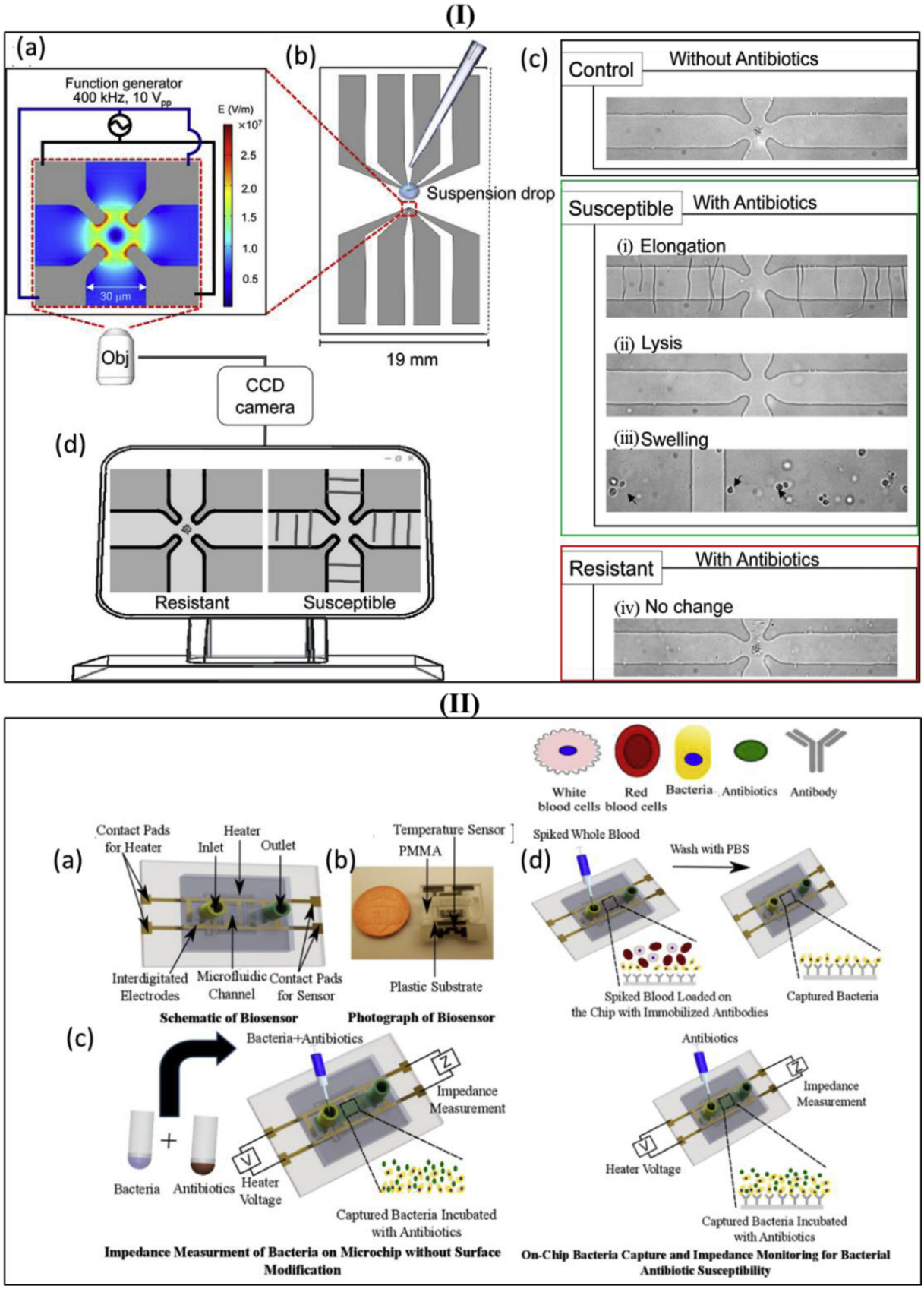

Fig. 11. (I) (a) Typical electric field distribution of a quadruple electrode array used in dielectrophoresis method-based AST application, (b) Schematic representation of dielectrophoretic AST device, (c) Typical behavior of suspension while doing AST, (d) Image of bacteria in resistant and susceptible mode. Reprinted with permission from (Su et al., 2017) Copyright (2017) American Chemical Society. Fig. 11(II) (a) Schematic representation of impedance biosensor with interdigitated electrodes, heater, and PMMA microfluidic channel for AST application, (b) Image of the device, (c) AST measurement using label-free electrical sensing on a biosensor without surface modification, (d) AST measurement using same biosensor with surface modification. Reprinted with permission from (Safavieh et al., 2017) Copyright (2017) American Chemical Society.

(Niyomdecha et al., 2017). This 3-APBA on a polytyramine (Pty) coated gold electrode enables reusability of the device and thus multiple bacteria were tested with the same device after washing with an acidic buffer. Under the influence of antibiotics binding of the number of bacteria to the 3-APBA was affected thereby changing the total capacitance measured. This reusable sensing device produced AST results in 2.5 h and was reused for 35 times successfully thus making it a potential candidate for developing a future diagnostic tool. In 2012, Puttaswamy et al. have developed a microfluidic channel with electrodes for AST applications (Puttaswamy et al., 2012). By measuring the capacitance of the suspension, the viability of bacterial cells under the influence of antibiotics was tested. In this case, the impedance of the bacterial suspension was measured at 500 different frequencies to determine charge-polarization of living and dead cell membranes. The highlight of this work was that it could determine MIC in 4 h and provide information about the antibiotic influenced bactericidal or bacteriostatic activity. One major limitation of this method was that the loading of suspension for each measurement makes it labour-intensive. Recently, Safavieh et al. have used microfluidics-based impedance analyser to test AST on *E. coli* and MRSA against gentamicin, methicillin, ampicillin, ciprofloxacin, erythromycin, and daptomycin antibiotics (Safavieh et al., 2017). In this study, silver electrodes for impedance measurement and carbon microheater for temperature stabilization were fabricated on a low-cost plastic substrate as shown in Fig. 11(II). A closed microchannel was formed by attaching an engraved poly(methyl methacrylate) (PMMA) sheets on the plastic substrate that carried the channel design. This microchip was functionalized with Anti-MRSA antibody to capture MRSA from the blood sample. The electrical impedance of the bacterial suspension was monitored at frequency 1 kHz at 1V in the presence and absence of antibiotics in both functionalized as well as non-functionalized conditions to test the efficacy of the chip for affinity-based and antibody-capture based sensing. This device provided AST results in less than 90 min thus making it a potential point-of-care technology for diagnosing patients suffering from UTI. Recently, Zhang et al. have developed a unique AST technique based on a multichannel capacitively coupled contactless conductivity detector (C4D) which the team termed as electrical bacterial growth sensor (EBGS) (Zhang et al., 2018). In C4D, the contactless conductivity of the suspension was measured, which was proportional to the concentration and mobility of the ionic charge carriers in the suspension. This EBGS system measured the conductivity of *E. coli* suspensions at the excitation frequency of 2.0 MHz at 16 V amplitude. The conductivity of bacterial solutions in the presence of chloramphenicol, penicillin G, and malachite green was monitored over incubation time. This sensor was also monitored online. In addition to the inherent advantages of electrochemical sensing techniques, this method provided more utilities such as freedom from polarization and elimination of passivation risks.

4. Conclusion

The engineering technologies for AST discussed in this article will help in reducing sample volumes, testing duration, improve sensitivity up to the level of a single bacterial cell, and potentially improve the portability of the overall system. Some of the emerging technologies such as mechanical, magnetic, and optical sensing-based methods are highly sensitive but are limited by the complexity and cost of the system. With advanced optical imaging techniques, researchers have studied AST on single bacterial cells. These bacteria cells were captured by physical confinement, dielectrophoresis, and/or agarose gel. On the other hand, different mechanical methods such as asynchronous magnetic bead rotation and cantilever fluctuation have been used to study AST on bacterial colonies as well as single cells. The microfluidics-based technologies provide several advantages as it require extremely low sample volumes and provide high throughput enabling parallel testing against multiple antibiotics. The efficiency of AST profiling improved significantly when a combination of optical, mechanical, and electrical modalities was integrated with microfluidics. Different microfluidic technologies such as gradient, droplet, and multiplexing enables testing with a wide variety of bacterial species and antibiotics in minimum time. These observations point to a trend that a multi-parametric sensing modality combining existing and emerging technologies will help improve the robustness of the systems. Emerging approaches such as data mining and machine learning combined with critical automation will hold the key for the next generation of AST systems. Considering the increasing trend of susceptible bacteria gaining resistance to conventional treatment, there will be added value in technologies that can clearly delineate between resistant, susceptible and persistent bacterial sample. This will pave the way for a more personalized treatment which will provide the best prognostic outcome.

However, from a translational point of view, the demonstration of the clinical value of these technologies is a critical aspect that is lacking in the literature. Except for the classical AST techniques and semi-automated systems, none of the emerging technologies discussed have gone through clearances by international bodies such as CLSI and EUCAST. Only a handful of studies have reported measurements from clinical patient samples or direct improvements in patient outcomes using their reported technology. While the scientific potential of these emerging technologies is immense and open up new and innovative ways of handling an important healthcare challenge, their adaptability into the existing clinical workflow and cost-effectiveness in comparison with gold standard techniques needs to be explored. The trend towards developing low-cost devices and point-of-care platforms is a positive step in this direction.

Conflict of interest

No conflict of interest exists.

Funding

No funding was received for this work.

CRediT authorship contribution statement

Bhagaban Behera: Data curation, Methodology, Writing - original draft. **G.K. Anil Vishnu:** Writing - original draft. **Suman Chatterjee:** Writing - original draft. **V.S.N. Sitaramgupta V:** Writing - original draft. **Niranjana Sreekumar:** Writing - original draft. **Apoorva Nagabhushan:** Writing - original draft. **Nirmala Rajendran:** Writing - original draft. **B.H. Prathik:** Writing - original draft. **Hardik J. Pandya:** Data curation, Methodology, Writing - original draft.

Acknowledgements

Bhagaban Behera acknowledges the Science and Engineering Research Board of Government of India for providing financial assistance (National Postdoctoral Fellowship, File number: PDF/2017/000644). Hardik J. Pandya acknowledges Indian Institute of Science, Bangalore for the start-up grant to establish the research and computational facilities at the Department of Electronic Systems Engineering. Hardik J. Pandya also acknowledges SERB (ECR/2017/001043) and Rajiv Gandhi University of Health Sciences (RGHUS)-Indian Institute of Science (IISc) collaborative project (RGUH0013) for providing financial assistance.

Appendix A. Supplementary data

Supplementary data to this article can be found online at https://doi.org/10.1016/j.bios.2019.111552.

References

Abdulhalim, I., Zourob, M., Lakhtakia, A., 2008. Electromagnetics 28, 214–242.
Adan, A., Alizada, G., Kiraz, Y., Baran, Y., Nalbant, A., 2017. Crit. Rev. Biotechnol. 37, 163–176.
Aghayee, S., Benadiba, C., Notz, J., Kasas, S., Dietler, G., Longo, G., 2013. J. Mol. Recognit. JMR 26, 590–595.
Alexander, B.D., Byrne, T.C., Smith, K.L., Hanson, K.E., Anstrom, K.J., Perfect, J.R., Reller, L.B., 2007. J. Clin. Microbiol. 45, 698–706.
Athamneh, A.I.M., Alajlouni, R.A., Wallace, R.S., Seleem, M.N., Senger, R.S., 2014. Antimicrob. Agents Chemother. 58, 1302–1314.
Avesar, J., Rosenfeld, D., Truman-Rosentsvit, M., Ben-Arye, T., Geffen, Y., Bercovici, M., Levenberg, S., 2017. Proc. Natl. Acad. Sci. 114, E5787–E5795.
Bai, H., Wang, R., Hargis, B., Lu, H., Li, Y., 2012. Sensors 12, 12506–12518.
Baker, C.N., Stocker, S.A., Culver, D.H., Thornsberry, C., 1991. J. Clin. Microbiol. 29, 533–538.
Balouiri, M., Sadiki, M., Ibnsouda, S.K., 2016a. J. Pharm. Anal. 6, 71–79.
Balouiri, M., Sadiki, M., Ibnsouda, S.K., 2016b. J. Pharm. Anal. 6, 71–79.
Baltekin, Ö., Boucharin, A., Tano, E., Andersson, D.I., Elf, J., 2017. Proc. Natl. Acad. Sci. 114, 9170–9175.
Baniukevic, J., Hakki Boyaci, I., Goktug Bozkurt, A., Tamer, U., Ramanavicius, A., Ramanaviciene, A., 2013. Biosens. Bioelectron. 43, 281–288.
Baraban, L., Bertholle, F., Salverda, M.L.M., Bremond, N., Panizza, P., Baudry, J., de Visser, J.A.G.M., Bibette, J., 2011. Lab Chip 11, 4057–4062.
Bauer, A.W., Kirby, W.M., Sherris, J.C., Turck, M., 1966. Am. J. Clin. Pathol. 45, 493–496.
Bauer, A.W., Perry, D.M., Kirby, W.M.M., 1959. AMA Arch. Intern. Med. 104, 208–216.
Belkum, A. van, Dunne, W.M., 2013. J. Clin. Microbiol. 51, 2018–2024.
Berghaus, L.J., Giguère, S., Guldbech, K., Warner, E., Ugorji, U., Berghaus, R.D., 2015. J. Clin. Microbiol. 53, 314–318.
Besant, J.D., Sargent, E.H., Kelley, S.O., 2015. Lab Chip 15, 2799–2807.
Bhalla, N., Jolly, P., Formisano, N., Estrela, P., 2016. 60, 1-8.
Bonkat, G., Solokhina, A., Rieken, M., Müller, G., Wyler, S., Gasser, T., Bachmann, A., 2013. Eur. Urol. Suppl. 12, e167.
Braff, W.A., Willner, D., Hugenholtz, P., Rabaey, K., Buie, C.R., 2013. PLoS One 8, e76751.
Braissant, O., Wirz, D., Göpfert, B., Daniels, A.U., 2009. FEMS Microbiol. Lett. 303, 1–8.
Campbell, J., McBeth, C., Kalashnikov, M., Boardman, A.K., Sharon, A., Sauer-Budge, A.F., 2016. Biomed. Microdevices 18, 103.
Cermak, N., Olcum, S., Delgado, F.F., Wasserman, S.C., Payer, K.R., Murakami, M.A., Knudsen, S.M., Kimmerling, R.J., Stevens, M.M., Kikuchi, Y., Sandikci, A., Ogawa, M., Agache, V., Baléras, F., Weinstock, D.M., Manalis, S.R., 2016. Nat. Biotechnol. 34, 1052–1059.
Chabot, V., Miron, Y., Charette, P.G., Grandbois, M., 2013. Biosens. Bioelectron. 50, 125–131.
Chaturvedi, V., Ramani, R., Pfaller, M.A., 2004. J. Clin. Microbiol. 42, 2249–2251.
Chen, C.H., Lu, Y., Sin, M.L.Y., Mach, K.E., Zhang, D.D., Gau, V., Liao, J.C., Wong, P.K., 2010. Anal. Chem. 82, 1012.
Chiang, Y.-L., Lin, C.-H., Yen, M.-Y., Su, Y.-D., Chen, S.-J., Chen, H.-F., 2009. Biosens. Bioelectron. 24, 1905–1910.
Choi, J., Jeong, H.Y., Lee, G.Y., Han, Sangkwon, Han, Shinhun, Jin, B., Lim, T., Kim, S., Kim, D.Y., Kim, H.C., Kim, E.-C., Song, S.H., Kim, T.S., Kwon, S., 2017. Sci. Rep. 7, 1148.
Choi, J., Jung, Y.-G., Kim, J., Kim, S., Jung, Y., Na, H., Kwon, S., 2013. Lab Chip 13, 280–287.
Choi, J., Yoo, J., Kim, K., Kim, E.-G., Park, K.O., Kim, Hyejin, Kim, Haeun, Jung, H., Kim, T., Choi, M., Kim, H.C., Ryoo, S., Jung, Y.-G., Kwon, S., 2016. Appl. Microbiol. Biotechnol. 100, 2355–2365.
Choi, J., Yoo, J., Lee, M., Kim, E.-G., Lee, J.S., Lee, S., Joo, S., Song, S.H., Kim, E.-C., Lee, J.C., Kim, H.C., Jung, Y.-G., Kwon, S., 2014. Sci. Transl. Med. 6 267ra174-267ra174.
Chotinantakul, K., Suginta, W., Schulte, A., 2014. Anal. Chem. 86, 10315–10322.
Chung, C.-C., Cheng, I.-F., Chen, H.-M., Kan, H.-C., Yang, W.-H., Chang, H.-C., 2012. Anal. Chem. 84, 3347–3354.
Chung, C.-C., Cheng, I.-F., Yang, W.-H., Chang, H.-C., 2011. Biomicrofluidics 5, 021102.
Chung, C.-Y., Wang, J.-C., Chuang, H.-S., 2016. PLoS One 11.
Churski, K., S. Kaminski, T., Jakiela, S., Kamysz, W., Baranska-Rybak, W., B. Weibel, D., Garstecki, P., 2012. Lab Chip 12, 1629–1637.
Citron, D.M., Ostovari, M.I., Karlsson, A., Goldstein, E.J., 1991. J. Clin. Microbiol. 29, 2197–2203.
Connell, J.L., Ritschdorff, E.T., Whiteley, M., Shear, J.B., 2013. Proc. Natl. Acad. Sci. 110, 18380–18385.
Cuenca-Estrella, M., Gomez-Lopez, A., Alastruey-Izquierdo, A., Bernal-Martinez, L., Cuesta, I., Buitrago, M.J., Rodriguez-Tudela, J.L., 2010. J. Clin. Microbiol. 48, 1782–1786.
Dai, J., Hamon, M., Jambovane, S., 2016. Bioengineering 3, 1–13.
Dai, J., Yoon, S.H., Sim, H.Y., Yang, Y.S., Oh, T.K., Kim, J.F., Hong, J.W., 2013. Anal. Chem. 85, 5892–5899.
Derzsi, L., S. Kaminski, T., Garstecki, P., 2016. Lab Chip 16, 893–901.
Du, W.-L., Xu, Y.-L., Xu, Z.-R., Fan, C.-L., 2008. Nanotechnology 19, 085707.
Eaton, P., Fernandes, J.C., Pereira, E., Pintado, M.E., Xavier Malcata, F., 2008. Ultramicroscopy 108, 1128–1134.
Eigner, U., Schmid, A., Wild, U., Bertsch, D., Fahr, A.-M., 2005. J. Clin. Microbiol. 43, 3829–3834.
Ertl, P., Robello, E., Battaglini, F., Mikkelsen, S.R., 2000. Anal. Chem. 72, 4957–4964.
Ertl, P., Wagner, M., Corton, E., Mikkelsen, S.R., 2003. Biosens. Bioelectron. 18, 907–916.
Espinel-Ingroff, A., Pfaller, M., Messer, S.A., Knapp, C.C., Killian, S., Norris, H.A., Ghannoum, M.A., 1999. J. Clin. Microbiol. 37, 591–595.
Etayash, H., Khan, M.F., Kaur, K., Thundat, T., 2016. Nat. Commun. 7, 12947.
Faria-Ramos, I., Espinar, M.J., Rocha, R., Santos-Antunes, J., Rodrigues, A.G., Cantón, R., Pina-Vaz, C., 2013. Clin. Microbiol. Infect. Off. Publ. Eur. Soc. Clin. Microbiol. Infect. Dis. 19, E8–E15.
Fernandes, J.C., Eaton, P., Gomes, A.M., Pintado, M.E., Xavier Malcata, F., 2009. Ultramicroscopy 109, 854–860.
Firdous, S., Anwar, S., Rafya, R., 2018. Laser Phys. Lett. 15, 065602.
France, D., Johnson, W., Cordell, W., Walls, F., 2016. Biophys. J. 110 200a.
Friedman, A., Blecher, K., Sanchez, D., Tuckman-Vernon, C., Gialanella, P., Friedman, J.M., Martinez, L.R., Nosanchuk, J.D., 2011. Virulence 2, 217–221.
Frígols, B., Martí, M., Salesa, B., Hernández-Oliver, C., Aarstad, O., Ulset, A.-S.T., Sætrom, G.I., Aachmann, F.L., Serrano-Aroca, Á., 2019. PLoS One 14, e0212819.
Funfak, A., Cao, J., Wolfbeis, O.S., Martin, K., Köhler, J.M., 2009. Microchim. Acta 164, 279–286.
Galvan, D.D., Yu, Q., 2018. Adv. Healthc. Mater. 7, 1701335.
Gauthier, C., St-Pierre, Y., Villemur, R., 2002. J. Med. Microbiol. 51, 192–200.
Gfeller, K.Y., Nugaeva, N., Hegner, M., 2005. Appl. Environ. Microbiol. 71, 2626–2631.
Godin, M., Delgado, F.F., Son, S., Grover, W.H., Bryan, A.K., Tzur, A., Jorgensen, P., Payer, K., Grossman, A.D., Kirschner, M.W., Manalis, S.R., 2010. Nat. Methods 7, 387–390.
Gupta, P., Khare, V., Kumar, D., Ahmad, A., Banerjee, G., Singh, M., 2015. J. Clin. Diagn. Res. JCDR 9, DC04–DC07.
Hadjigeorgiou, K., Kastanos, E., Pitris, C., 2016. IEEE Healthcare Innovation Point-Of-Care Technologies Conference. HI-POCT, pp. 158–161.
He, J., Mu, X., Guo, Z., Hao, H., Zhang, C., Zhao, Z., Wang, Q., 2014. Eur. J. Clin. Microbiol. Infect. Dis. 33, 2223–2230.
Heesemann, J., 1993. Infection 21 (Suppl. 1), S4–S9.
Hou, Z., An, Y., Hjort, Karin, Hjort, Klas, Sandegren, L., Wu, Z., 2014a. Lab Chip 14, 3409–3418.
Hou, Z., An, Y., Hjort, Karin, Hjort, Klas, Sandegren, L., Wu, Z., 2014b. Lab Chip 14, 3409–3418.
Howell, M., Wirz, D., Daniels, A.U., Braissant, O., 2012. J. Clin. Microbiol. 50, 16–20.
Huang, T.-H., Ning, X., Wang, X., Murthy, N., Tzeng, Y.-L., Dickson, R.M., 2015. Anal. Chem. 87, 1941–1949.
J. Cira, N., Y. Ho, J., E. Dueck, M., B. Weibel, D., 2012. Lab Chip 12, 1052–1059.
Jepras, R.I., Paul, F.E., Pearson, S.C., Wilkinson, M.J., 1997. Antimicrob. Agents Chemother. 41, 2001–2005.
Jiang, L., Boitard, L., Broyer, P., Chareire, A.-C., Bourne-Branchu, P., Mahé, P., Tournoud, M., Franceschi, C., Zambardi, G., Baudry, J., Bibette, J., 2016. Eur. J. Clin. Microbiol. Infect. Dis. 35, 415–422.
Jo, N., Kim, B., Lee, S.-M., Oh, J., Park, I.H., Jin Lim, K., Shin, J.-S., Yoo, K.-H., 2018. Biosens. Bioelectron. 102, 164–170.
Johannessen, E.A., Weaver, J.M.R., Cobbold, P.H., Cooper, J.M., 2002. IEEE Trans. NanoBioscience 1, 29–36.
Johari, J., Hübner, Y., Hull, J.C., Dale, J.W., Hughes, M.P., 2003. Phys. Med. Biol. 48 N193.
Johnson, W.L., France, D.C., Rentz, N.S., Cordell, W.T., Walls, F.L., 2017. Sci. Rep. 7, 12138.
Jorgensen, J.H., Ferraro, M.J., 2009. Clin. Infect. Dis. Off. Publ. Infect. Dis. Soc. Am. 49, 1749–1755.
Kalashnikov, M., Campbell, J., Lee, J.C., Sharon, A., Sauer-Budge, A.F., 2014. JoVE J. Vis. Exp, e50828.
Kalashnikov, M., Lee, J.C., Campbell, J., Sharon, A., Sauer-Budge, A.F., 2012. Lab Chip 12, 4523–4532.
Kalashnikov, M., Lee, J.C., Sauer-Budge, A.F., 2018. Diagnostics 8, 24.
Kalashnikov, M., Mueller, M., McBeth, C., Lee, J.C., Campbell, J., Sharon, A., Sauer-Budge, A.F., 2017. Sci. Rep. 7, 8031.
Kaminski, T.S., Scheler, O., Garstecki, P., 2016. Lab Chip 16, 2168–2187.
Kara, V., Duan, C., Gupta, K., Kurosawa, S., J. Stearns-Kurosawa, D., L. Ekinci, K., 2018. Lab Chip 18, 743–753.
Kasas, S., Ruggeri, F.S., Benadiba, C., Maillard, C., Stupar, P., Tournu, H., Dietler, G., Longo, G., 2015. Proc. Natl. Acad. Sci. U. S. A. 112, 378–381.
Kastanos, E.K., Kyriakides, A., Hadjigeorgiou, K., Pitris, C., 2010. J. Raman Spectrosc. 41, 958–963.
Kaushik, A.M., Hsieh, K., Chen, L., Shin, D.J., Liao, J.C., Wang, T.-H., 2017. Biosens. Bioelectron. 97, 260–266.
Kee, J.S., Lim, S.Y., Perera, A.P., Zhang, Y., Park, M.K., 2013. Sens. Actuators B Chem. 182, 576–583.
Khatoon, U.T., Nageswara Rao, G.V.S., Mohan, K.M., Ramanaviciene, A., Ramanavicius, A., 2017. Vacuum 146, 259–265.
Kim, S.C., Cestellos-Blanco, S., Inoue, K., Zare, R.N., 2015. Antibiotics 4, 455–466.
Kinnunen, P., Carey, M.E., Craig, E., Brahmasandra, S.N., McNaughton, B.H., 2014. Sens. Actuators B Chem. 190, 265–269.
Kinnunen, P., McNaughton, B.H., Albertson, T., Sinn, I., Mofakham, S., Elbez, R., Newton, D.W., Hunt, A., Kopelman, R., 2012. Small 8, 2477–2482.
Kinnunen, P., Sinn, I., McNaughton, B.H., Newton, D.W., Burns, M.A., Kopelman, R., 2011. Biosens. Bioelectron. 26, 2751–2755.
Knudsen, S.M., von Muhlen, M.G., Schauer, D.B., Manalis, S.R., 2009. Anal. Chem. 81, 7087–7090.
Kong, K.-F., Schneper, L., Mathee, K., 2010. APMIS Acta Pathol. Microbiol. Immunol. Scand. 118, 1–36.
Lang, H.P., Gerber, C., 2008. Microcantilever sensors. In: STM and AFM Studies on (Bio) Molecular Systems: Unravelling the Nanoworld, Topics in Current Chemistry. Springer, Berlin, Heidelberg, pp. 1–27.
Lee, W., Fon, W., Axelrod, B.W., Roukes, M.L., 2009. Proc. Natl. Acad. Sci. 106,

15225–15230.
Lee, W., You, M., Wei, P., Chung, P., Lee, K., Tian, W., 2015. IEEE Sensors 1–4.
Leester-Schädel, M., Lorenz, T., Jürgens, F., Richter, C., 2016. Springer, Cham, pp. 23–57.
Leonard, H., Halachmi, S., Ben-Dov, N., Nativ, O., Segal, E., 2017. ACS Nano 11, 6167–6177.
Lewis, G., Daniels, A.U. (Dan), 2003. J. Biomed. Mater. Res. B Appl. Biomater. 66B, 487–501.
Li, B., Qiu, Y., Glidle, A., McIlvenna, D., Luo, Q., Cooper, J., Shi, H.-C., Yin, H., 2014. Anal. Chem. 86, 3131–3137.
Lissandrello, C., Inci, F., Francom, M., Paul, M.R., Demirci, U., Ekinci, K.L., 2014. Appl. Phys. Lett. 105.
Liu, C.-Y., Han, Y.-Y., Shih, P.-H., Lian, W.-N., Wang, H.-H., Lin, C.-H., Hsueh, P.-R., Wang, J.-K., Wang, Y.-L., 2016. Sci. Rep. 6, 23375.
Liu, T.-T., Lin, Y.-H., Hung, C.-S., Liu, T.-J., Chen, Y., Huang, Y.-C., Tsai, T.-H., Wang, H.-H., Wang, D.-W., Wang, J.-K., Wang, Y.-L., Lin, C.-H., 2009. PLoS One 4, e5470.
Liu, Z., Sun, H., Ren, K., 2017. ChemPlusChem 82, 792–801.
Long, Z., Nugent, E., Javer, A., Cicuta, P., Sclavi, B., Cosentino Lagomarsino, M., Dorfman, K.D., 2013. Lab Chip 13, 947–954.
Longo, G., Alonso-Sarduy, L., Rio, L.M., Bizzini, A., Trampuz, A., Notz, J., Dietler, G., Kasas, S., 2013. Nat. Nanotechnol. 8, 522–526.
Longo, G., Kasas, S., 2014. Wiley Interdiscip. Rev. Nanomed. Nanobiotechnol. 6, 230–244.
Lu, Y., Gao, J., Zhang, D.D., Gau, V., Liao, J.C., Wong, P.K., 2013. Anal. Chem. 85, 3971–3976.
Luo, X., J. Davis, J., 2013. Chem. Soc. Rev. 42, 5944–5962.
Ma, F., Rehman, A., Sims, M., Zeng, X., 2015. Anal. Chem. 87, 4385–4393.
Malmberg, C., Yuen, P., Spaak, J., Cars, O., Tängdén, T., Lagerbäck, P., 2016. PLoS One 11, e0167356.
Mann, T.S., Mikkelsen, S.R., 2008. Anal. Chem. 80, 843–848.
Martinez-Perdiguero, J., Retolaza, A., Otaduy, D., Juarros, A., Merino, S., 2013. Sensors 13, 13960–13968.
Matsumoto, Y., Sakakihara, S., Grushnikov, A., Kikuchi, K., Noji, H., Yamaguchi, A., Iino, R., Yagi, Y., Nishino, K., 2016. PLoS One 11.
Mehrotra, P., 2016. J. Oral Biol. Craniofacial Res. 6, 153–159.
Mittman, S.A., Huard, R.C., Della-Latta, P., Whittier, S., 2009. J. Clin. Microbiol. 47, 3557–3561.
Mohan, R., Mukherjee, A., Sevgen, S.E., Sanpitakseree, C., Lee, J., Schroeder, C.M., Kenis, P.J.A., 2013. Biosens. Bioelectron. 49, 118–125.
Mohan, R., Sanpitakseree, C., V. Desai, A., E. Sevgen, S., M. Schroeder, C., A. Kenis, P.J., 2015. RSC Adv. 5, 35211–35223.
Moritz, T.J., Polage, C.R., Taylor, D.S., Krol, D.M., Lane, S.M., Chan, J.W., 2010a. J. Clin. Microbiol. 48, 4287–4290.
Moritz, T.J., Taylor, D.S., Polage, C.R., Krol, D.M., Lane, S.M., Chan, J.W., 2010b. Anal. Chem. 82, 2703–2710.
Munita, J.M., Arias, C.A., 2016. Micro. Spectr. 4, 1–24.
Nath, N., Chilkoti, A., 2004. Anal. Chem. 76, 5370–5378.
Nawattanapaiboon, K., Kiatpathomchai, W., Santanirand, P., Vongsakulyanon, A., Amarit, R., Somboonkaew, A., Sutapun, B., Srikhirin, T., 2015. Biosens. Bioelectron. 74, 335–340.
Nazemi, E., Hassen, W.M., Frost, E.H., Dubowski, J.J., 2017. Biosens. Bioelectron. 93, 234–240.
Nemeth, J., Oesch, G., Kuster, S.P., 2015. J. Antimicrob. Chemother. 70, 382–395.
Niyomdecha, S., Limbut, W., Numnuam, A., Asawatreratanakul, P., Kanatharana, P., Thavarungkul, P., 2017. Biosens. Bioelectron. 96, 84–88.
Nseir, S., Povoa, P., 2015. Intensive Care Med. 41, 531–533.
Onishi, K., Enomoto, J., Araki, T., Takagi, R., Suzuki, H., Fukuda, J., 2018. Analyst 143, 396–399.
Peitz, I., van Leeuwen, R., 2010. Lab Chip 10, 2944–2951.
Pilát, Z., Bernatová, S., Ježek, J., Kirchhoff, J., Tannert, A., Neugebauer, U., Samek, O., Zemánek, P., 2018. Sensors 18.
Piliarik, M., Vaisocherová, H., Homola, J., Rasooly, A., Herold, K.E. (Eds.), 2009. Biosensors and Biodetection, Methods in Molecular Biology™. Humana Press, Totowa, NJ, pp. 65–88.
Pil Kim, K., Kim, Y.-G., Choi, C.-H., Kim, H.-E., Lee, S.-H., Chang, W.-S., Lee, C.-S., 2010. Lab Chip 10, 3296–3299.
Premasiri, W.R., Chen, Y., Williamson, P.M., Bandarage, D.C., Pyles, C., Ziegler, L.D., 2017. Anal. Bioanal. Chem. 409, 3043–3054.
Puttaswamy, S., Gupta, S.K., Regunath, H., Smith, L.P., Sengupta, S., 2018. Arch. Clin. Microbiol. 9.
Puttaswamy, S., Lee, B.-D., Amighi, B., Chakraborty, S., Sengupta, S., 2012. J. Biosens. Bioelectron. 4, 1–6.
Q. Boedicker, J., Li, L., R. Kline, T., F. Ismagilov, R., 2008. Lab Chip 8, 1265–1272.
Ramani, R., Ramani, A., Wong, S.J., 1997. J. Clin. Microbiol. 35, 2320–2324.
Ran, M., Wang, Y., Wang, S., Luo, C., 2015. Biomed. Microdevices 17, 67.
Read, A.F., Woods, R.J., 2014. Evol. Med. Public Health 147.
Reller, L.B., Weinstein, M., Jorgensen, J.H., Ferraro, M.J., 2009a. Clin. Infect. Dis. 49, 1749–1755.
Reller, L.B., Weinstein, M., Jorgensen, J.H., Ferraro, M.J., 2009b. Clin. Infect. Dis. 49, 1749–1755.
Reller, L.B., Weinstein, M., Jorgensen, J.H., Ferraro, M.J., 2009c. Clin. Infect. Dis. 49, 1749–1755.
Rowat, A.C., Bird, J.C., Agresti, J.J., Rando, O.J., Weitz, D.A., 2009. Proc. Natl. Acad. Sci. U. S. A. 106, 18149–18154.
Sabhachandani, P., Sarkar, S., Zucchi, P.C., Whitfield, B.A., Kirby, J.E., Hirsch, E.B., Konry, T., 2017. Microchim. Acta 184, 4619–4628.
Safavieh, M., Pandya, H.J., Venkataraman, M., Thirumalaraju, P., Kanakasabapathy, M.K., Singh, A., Prabhakar, D., Chug, M.K., Shafiee, H., 2017. ACS Appl. Mater. Interfaces 9, 12832–12840.
Saint-Ruf, C., Crussard, S., Franceschi, C., Orenga, S., Ouattara, J., Ramjeet, M., Surre, J., Matic, I., 2016. Front. Microbiol. 7.
Samadi, A., Zhang, C., Chen, J., Reihani, S.N.S., Chen, Z., 2015. Biomed. Opt. Express 6, 112–117.
Saravanan, M., Ramachandran, B., Barabadi, H., 2018. Microb. Pathog. 114, 180–192.
Schofield, C.B., 2012. Am. Soc. Clin. Lab. Sci. 25, 233–239.
Sinn, I., Albertson, T., Kinnunen, P., Breslauer, D.N., McNaughton, B.H., Burns, M.A., Kopelman, R., 2012. Anal. Chem. 84, 5250–5256.
Sinn, I., Kinnunen, P., Albertson, T., McNaughton, B.H., Newton, D.W., Burns, M.A., Kopelman, R., 2011. Lab Chip 11, 2604–2611.
Snyder, J.W., Munier, G.K., Johnson, C.L., 2008. J. Clin. Microbiol. 46, 2327–2333.
Soltani, R., Ehsanpoor, M., Khorvash, F., Shokri, D., 2014. J. Res. Pharm. Pract. 3, 6.
Su, I.-H., Ko, W.-C., Shih, C.-H., Yeh, F.-H., Sun, Y.-N., Chen, J.-C., Chen, P.-L., Chang, H.-C., 2017. Anal. Chem. 89, 4635–4641.
Sun, H., Liu, Z., Hu, C., Ren, K., 2016. Lab Chip 16, 3130–3138.
Syal, K., Iriya, R., Yang, Y., Yu, H., Wang, S., Haydel, S.E., Chen, H.-Y., Tao, N., 2016. ACS Nano 10, 845–852.
Syal, K., Mo, M., Yu, H., Iriya, R., Jing, W., Guodong, S., Wang, S., Grys, T.E., Haydel, S.E., Tao, N., 2017a. Theranostics 7, 1795–1805.
Syal, K., Shen, S., Yang, Y., Wang, S., Haydel, S.E., Tao, N., 2017b. ACS Sens. 2, 1231–1239.
Tafin, U.F., Clauss, M., Hauser, P.M., Bille, J., Meis, J.F., Trampuz, A., 2012. Clin. Microbiol. Infect. 18, E241–E245.
Takagi, R., Fukuda, J., Nagata, K., Yawata, Y., Nomura, N., Suzuki, H., 2013. Analyst 138, 1000–1003.
Tan, S., Tatsumura, Y., 2015. Alexander Fleming (1881–1955): discoverer of penicillin. Singap. Med. J. 56, 366–367.
Tang, M., Huang, X., Chu, Q., Ning, X., Wang, Y., Kong, S.-K., Zhang, X., Wang, G., Ho, H.-P., 2018. Lab Chip 18, 1452–1460.
Tang, Y., Zhen, L., Liu, J., Wu, J., 2013. Anal. Chem. 85, 2787–2794.
Tawil, N., Mouawad, F., Lévesque, S., Sacher, E., Mandeville, R., Meunier, M., 2013. Biosens. Bioelectron. 49, 334–340.
Tracy, B.P., Gaida, S.M., Papoutsakis, E.T., 2010. Curr. Opin. Biotechnol. Anal. Biotechnol. 21, 85–99.
Turner, A.P.F., 2013. Chem. Soc. Rev. 42, 3184–3196.
van Belkum, A., Dunne, W.M., 2013. J. Clin. Microbiol. 51, 2018–2024.
van Herwaarden, A.W., 2005. In: 8th Lähnwitzseminar on Calorimetry, vol 432. pp. 192–201.
Vigneshvar, S., Sudhakumari, C.C., Senthilkumaran, B., Prakash, H., 2016. Bioeng. Biotechnol. 4.
von Ah, U., Wirz, D., Daniels, A.U., 2009. BMC Microbiol. 9, 106.
Walter, A., Reinicke, M., Bocklitz, T., Schumacher, W., Rösch, P., Kothe, E., Popp, J., 2011. Anal. Bioanal. Chem. 400, 2763–2773.
Weibull, E., Antypas, H., Kjäll, P., Brauner, A., Andersson-Svahn, H., Richter-Dahlfors, A., 2014. J. Clin. Microbiol. 52, 3310–3317.
White, R.L., Burgess, D.S., Manduru, M., Bosso, J.A., 1996. Antimicrob. Agents Chemother. 40, 1914–1918.
Whitesides, G.M., 2006. Nature 442, 368–373.
Yanase, Y., Hiragun, T., Ishii, K., Kawaguchi, T., Yanase, T., Kawai, M., Sakamoto, K., Hide, M., 2014. Sensors 14, 4948–4959.
Zhang, X., Jiang, X., Yang, Q., Wang, X., Zhang, Y., Zhao, J., Qu, K., Zhao, C., 2018. Anal. Chem. 90, 6006–6011.